Chapter-4

Texturization of protein isolated from Manila tamarind seeds using freeze texturization and freeze structuring and comparison of its textural characteristics with texturized soy protein

4.1.Introduction

The demand for meat is skyrocketing annually as billions of people worldwide are consuming staggering amounts of it daily. This insatiable demand is sustained by a vast network of slaughterhouses and animal farms. However, to fulfil the requirements of our burgeoning world population in the upcoming years, significant increases in meat production are imperative. Yet, this amount of heightened production comes at a steep environmental cost. Animal agriculture contributes to land and water degradation, pollution, greenhouse gas emissions, and excessive energy consumption (Arora et al., 2023). Beyond environmental concerns, ethical issues surrounding animal welfare and public health risks also weigh heavily in the debate over meat consumption. Although awareness of the health hazards linked to meat consumption is growing, only a fraction of the global populace has embraced vegetarianism as a viable alternative (Dekkers et al., 2018). Recent years have seen increased interest in plant-based meat substitutes due to concerns about the sustainability of animal protein production amid growing global populations and limited natural resources (Yuliarti et al., 2021). These plant-based meat alternatives aim to match conventional meat in dietary function, sensory attributes, and nutritional value. The market for plant-based meat has expanded to meet consumer demand and ensure long-term food supply sustainability, with research efforts intensifying globally, particularly in Asia. For plant-based meat substitutes to succeed, they must closely mimic meat in taste and texture, as these factors significantly influence meat-eaters' willingness to modify their diets (Sha & Xiong, 2020). Researchers are focusing on replicating key structural characteristics of meat, such as muscle fiber capillarity for water retention and texture (Tuorila & Hartmann, 2020).

The majority of vegetable proteins are employed as food components as protein isolates or concentrates, whose manufacturing techniques may alter their functional characteristics and thus restrict their application. Presently, America, the Philippines,

Southern Florida, Cuba, the Caribbean, Hawaii, India, Bangladesh, and East Africa are among the regions with a large distribution of Manila tamarind (*Pithecellobium dulce*) plant (Rao, 2013). The pulp of the Manila tamarind fruit is eaten raw, and seeds can be roasted, or used to make sour-sweet beverages like lemonade. Despite the fact that Manila tamarind seeds can supply up to 39% of proteins in the form of flour, which can be recovered as protein isolate, they are typically thrown away, losing their nutritional value (Rao et al., 2011). Various methods have been developed to simulate desirable structural features in plant-based meat, with a focus on achieving textures similar to muscle fibers, particularly chewiness (Sha & Xiong, 2020). Freeze-texturization is a cutting-edge method that creates fibrous, meat-like structures while using low temperatures to retain nutrients like vitamins and proteins. It also preserves moisture, improving the juiciness and sensory qualities of plant-based meat alternatives compared to traditional high-heat extrusion (Sha & Xiong, 2020; Yuliarti et al., 2021). Traditional techniques like thermomechanical extrusion and shear have shown some success, though the resulting aggregates of plant proteins do not microscopically resemble the anisotropic structure of muscle fibers, often leading to customer dissatisfaction regarding dryness or lack of juiciness (Dekkers et al., 2018; Yuliarti et al., 2021). Extrusion is a widely used method in large-scale production, with properties influenced by factors like screw type, speed, temperature, and pressure (Dekkers et al., 2018). Adjustments to molding temperature and moisture content can further affect characteristics such as water absorption, color, and texture (Yuliarti et al., 2021). Despite the prominence of extrusion, alternative methods like spinning techniques and 3D food printing are being explored to create more realistic meat analogues, though they still face challenges in cost and texture refinement (Chantanuson et al., 2022).

The process of freeze-structuring consists of creating a distinct fibrous structure by freezing a protein emulsion. The process of removing ice crystals leaves behind a fibrous and porous microstructure identical to the meat of animal muscles, which are composed of many sheet-like proteins that are tightly connected in parallel (Yuliarti et al., 2021). The plant protein source that is employed has a significant impact on the creation of fibrous structures of the meat analogues utilizing the freeze-structuring approach. This is due to the possibility that different protein sources have distinct structure-function correlations concerning texture creation, gelation, and hydration and solubility, all of which affect how the meat mimic is ultimately structured (Dekkers et al., 2018; Yuliarti

et al., 2021). In developing plant-based meat alternatives, a variety of functional ingredients are crucial for replicating the characteristics of animal protein-based products. The use of unripe jackfruit as a component in meat analogues not only helps provide nutritious dietary fiber but also increases the value of local agricultural products and reduces waste from the jackfruit harvest. Unripe jackfruit helps in improving the microstructure of chicken meat analogues and provides better texture characteristics exhibiting anisotropic (layered or fibrous) structures when used in combination with other ingredients such as wheat gluten and plant protein isolates (Taikerd & Leelawat, 2023). Carbohydrate polymers like seaweed-derived alginates are commonly used to improve texture uniformity, retain moisture, and prevent syneresis (Sha & Siong, 2020). Liquid ingredients such as water and oils play essential roles in hydrating components like textured vegetable protein, facilitating cohesion, and mimicking meat juiciness while also infusing flavors (Kyriakopoulou et al., 2019; El Youssef et al., 2020). Salt serves multiple functions, including enhancing flavor, intensifying taste profiles, and contributing to savory notes typical of meat. It also aids in texture modulation by increasing protein solubility and moisture retention, thereby improving the succulence and tenderness of the meat analogues. This combination of ingredients and their interactions is key to creating plant-based alternatives that closely resemble traditional meat products in texture, appearance, taste, and mouthfeel (Arora et al., 2023).

The objective of this research was to optimize the composition of different components suitable for structuring and identifying an appropriate mixture composition to achieve this goal and develop a fibrous structure using freeze texturization and freeze-structuring technique. Different concentrations of proteins and other ingredients were employed to produce the texturized protein, which were subsequently evaluated based on their structural and physicochemical attributes, including textural and visual characteristics. The texturizing conditions were carefully controlled to create a highly anisotropic structure from plant-based proteins, comparable to that of cooked animal muscle tissue. The outcomes of this study have the potential to facilitate the broader adoption of plant-based protein as substitutes in place of animal-derived products.

4.2.Materials and methods

4.2.1. Materials

Manila tamarind seeds were collected from a local town in Uttar Pradesh, India. Sunflower oil, raw jackfruit and wheat gluten were purchased from the local market of Tezpur, Assam, India.

4.2.2. Chemicals and reagents

Hexane (bp ~ 69 °C), sodium alginate, calcium chloride and the remaining food-grade and analytical grade substances used in the analysis were all purchased from Octagon Chemicals & Instruments, Zenith India, Guwahati, Assam, India.

4.2.3. Preparation of jackfruit flour

Raw jackfruit samples were sliced into slabs that were of identical thickness (10 mm). The jackfruit slabs were then dried using a cabinet tray dryer. The jackfruit slabs were spread out over the cabinet dryer trays and dried for 10 h at 60 °C. The flesh of the dried jackfruit was subsequently ground using a grinder (Agrosa Ltd., India) and passed through a sieve (mesh number 60) to obtain flour of uniform size. After that, jackfruit flour was kept in polythene bags for further usage (Sharma et al., 2019).

4.2.4. Preparation of Protein Isolates

The Manila tamarind seeds were ground into a uniform flour size using a stone mill, and the mixture was subsequently sieved through a 60-mesh screen. Proteins were recovered from defatted Manila tamarind seed flour using the protocol of López et al. (2018). To create a slurry, a suspension of the flour in distilled water (DW) (1:3) was made, and it was stirred for 60 min. To extract protein, the slurry's pH was kept at 12 using 2 M NaOH, and stirring was done for 30 min. Following the stirring process, the slurry was centrifuged for 20 min at 7000×g to obtain the supernatant. The proteins were precipitated from the supernatant by adjusting its pH to 4 with 1 M HCl. The mixture was centrifuged once again for 20 min at 7000×g, and the protein pellet was obtained by discarding the supernatant. The pellets were centrifuged for 20 min at 7000×g after being rinsed two or three times with DW. After being cleaned, the pellets were frozen, freeze-dried, and stored for later use.

4.2.5. Optimization of ingredients for production of texturized protein

Each of the solid ingredients Manila tamarind seed protein (PI), wheat gluten (WG), raw jackfruit flour (JFF), sodium alginate (SA), and common salt (S) were mixed as per the quantity mentioned in experimental design to create suspensions of the solid phase with various solid components. To create the liquid phase (L), sunflower oil and water were combined at a weight ratio of 1:10 **(Table 4.1)** and the solid phase ingredients were mixed with the liquid phase and the resulting liquid mixture was homogenized using high pressure homogenizer at 10000 rpm for 10 min to form stable suspension.

Table 4.1: Different mixture components of the experimental design with their minimum and maximum values used in the formulation of freeze texturized protein

Components of the mixture design	Name of ingredients used	Units	Minimum quantity used	Maximum quantity used
A	PI	%	4.61	6.53
B	WG	%	0.77	1.33
C	JFF	%	0.38	1.15
D	SA	%	0	3.6
E	S	%	0	1.8
F	L	%	86.02	94.24
			Total =	100.00

PI-Manila tamarind seed protein, WG-wheat gluten, JFF-raw jackfruit flour, SA-sodium alginate, S-common salt, and L-liquid (sunflower oil and water in 1:10)

4.2.6. Experimental design for optimization of ingredient composition

In this research, the mixture components (Manila tamarind seed protein (PI), wheat gluten (WG), raw jackfruit flour (JFF), sodium alginate (SA), common salt (S), liquid (L)) to be used for the formulation of texturized protein were optimized **(Table 4.2)**. The Design-Expert software was used to determine the optimum proportions for the texturized protein formulation. All the mixture component proportions are subject to constraints. As a result, a D-optimal mixture design was used, however with certain limitations. The design of this experiment was based on six components consisting of PI, WG, JFF, SA, S and L with the sum of the component proportion of 100% **(Table 4.1)**.

Table 4.2: List of all the dependent and independent variables with the response values

Run	Components (Independent variables)						Responses (Dependent variables)			
	A:PI	B:WG	C:JFF	D:SA	E:S	F:L	Hardness	Springiness	Fibre	Protein
Units	%	%	%	%	%	%	(g)		(% d.b.)	(% d.b.)
1	5.35	0.83	1.15	0.91	1.41	90.35	333.41	0.444	2.62	51.89
2	5.68	1.02	0.71	1.92	0	90.67	577.8	0.836	1.82	56.17
3	4.69	0.99	0.68	0	0.76	92.88	114.06	0.737	1.7	47.66
4	6.53	0.9	1.15	3.6	1.8	86.02	215.59	0.523	2.77	65.71
5	5.68	1.02	0.71	1.92	0	90.67	523.95	0.957	1.82	56.38
6	5.92	0.77	0.38	0	1.8	91.13	119.24	0.138	0.88	55.92
7	6.22	1.27	1.15	2.21	0.58	88.57	497.34	0.83	2.7	66.02
8	6.22	1.27	1.15	2.21	0.58	88.57	440.7	0.764	2.7	65.96
9	6.53	1.33	0.38	3.6	0	88.16	187.27	0.241	0.92	66.15
10	4.61	1.33	1.15	0	0	92.91	123.46	0.749	2.67	49.84
11	6.53	0.77	1.15	0	0	91.55	132.59	0.155	2.64	61.29
12	4.61	1.33	1.15	1.17	0	91.74	450.22	0.493	2.68	49.86
13	4.61	0.77	0.38	0	0	94.24	144.12	0.208	0.88	45.15
14	6.53	1.14	0.92	0	1.8	89.61	174.14	0.885	2.11	64.55
15	4.61	1.33	0.38	0.35	1.8	91.53	304.64	0.6	0.91	49.84
16	4.61	1.33	0.61	2.54	0.45	90.46	381.8	0.326	1.42	49.99
17	4.61	0.77	0.38	2.52	0	91.72	436.46	0.21	0.92	45.14
18	5.24	1.13	0.38	3.6	1.54	88.11	158.67	0.974	0.94	53.61
19	5.48	1.33	0.77	1.53	1.79	89.1	515.67	0.424	1.78	57.2
20	5.35	0.83	1.15	0.91	1.41	90.35	377.47	0.483	2.62	51.86
21	4.61	0.96	1.15	3.6	0	89.68	138.41	0.573	2.77	46.87
22	4.61	0.77	0.76	2.73	1.8	89.33	328.96	0.24	1.83	45.14
23	4.78	1.33	1.15	3.6	1.8	87.34	122.9	0.194	2.75	51.42
24	6.05	0.77	0.38	3.13	0	89.67	277.1	0.253	0.91	57.39
25	6.53	0.98	0.38	1.74	0.85	89.52	578.8	0.627	0.9	63.2
26	5.89	1.33	0.38	0	0.17	92.23	205.96	0.67	0.88	60.76
27	6.4	1.33	0.56	2.62	1.8	87.29	350.85	0.291	1.29	65.39
28	5.89	0.77	0.78	3.6	0.72	88.24	119.45	0.315	1.8	55.55
29	6.53	0.98	0.38	1.74	0.85	89.52	652.58	0.665	0.9	63.02
30	6.53	1.33	1.15	1.13	1.8	88.06	439.87	0.555	2.72	65.98
31	4.69	0.99	0.68	0	0.76	92.88	252.73	0.76	1.7	47.8

PI-Manila tamarind seed protein, WG-wheat gluten, JFF-raw jackfruit flour, SA-sodium alginate, S-common salt, and L-liquid

Design expert software designed 31 runs, of which 21 runs were different and 5 runs had two replicates **(Table 4.2)**. According to D-optimal approach, effect of these components on the properties (responses) of texturized protein was evaluated and then the optimum combination was determined. The mixture was then texturized through the freeze-texturization using the methodology of Chantanuson et al. (2022) as described in the next section **4.3.2.** The responses studied were Hardness (g), Springiness, fiber content (%), and protein content (%). The combination of elements which produced the best results was figured out based on the effect of each component. Based on high R-squared, low standard deviation, and low expected sum of squares, the optimal model was fitted. While the *p*-values of the models that were accepted were smaller than 0.05, the *p*-values indicating lack of fit were higher than 0.05.

4.2.7. Production of texturized protein by freeze texturization

The solid ingredients namely Manila tamarind seed protein (PI), wheat gluten (WG), raw jackfruit flour (JFF), sodium alginate (SA), and common salt (S) were mixed with the liquid phase (L), consisting of sunflower oil and water (at a weight ratio of 1:10) to produce a slurry. After homogenizing the resultant slurry, the combined samples were put into cubic silicone molds (3.5 × 3.5 × 3.5 cm). An insulator was placed on top and bottom of the molds, and they were frozen for eight h at -10 °C (1st freezing step). The frozen samples were taken out of the molds after 8 h, immersed in a 3% $CaCl_2$ solution, and allowed to stabilize at 4 ℃ for 12 h. The resulting gel was once more frozen in the same way as in the first step, for 8 h at -10 °C (2nd freezing step).

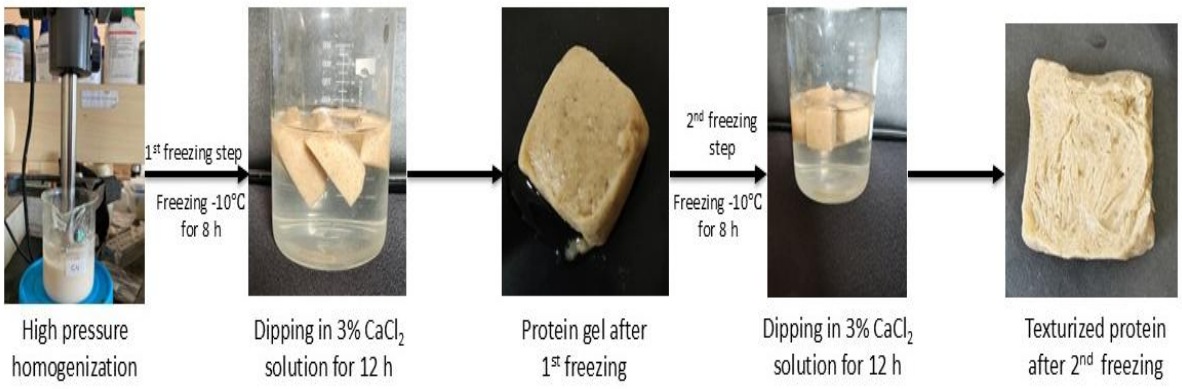

Figure 4.1: An overview of all the steps involved in the preparation of freeze texturized protein

All specimens were kept at 4 °C until further examination (Chantanuson et al., 2022). **Figure 4.1** gives an overview of all the steps involved in the preparation of freeze texturized protein.

4.2.8. Optimization of the parameters

Using Design Expert software, the desired outcomes for each variable and responses were chosen, and the numerical values of the independent variables and simultaneous optimization of the multiple responses were carried out. For the optimization of the process, the ingredients PI, WG, JFF, SA were kept at maximum while S and L were kept at minimum so as to obtain ingredient blend which produces texturized products with good physical and functional qualities. The pre-determined goal sets for responses were minimum values for hardness of the product. On the other hand, the product should also exhibit maximum values for springiness, fiber and protein content. To achieve the optimal solution for multiple responses, individual goals were combined into a composite function known as the desirability function. This objective function reflects a desirable value ranging from 0 to 1.

4.2.9. Production of texturized protein by freeze-structuring

The optimized formulation obtained from section **4.2.7** was further utilized for the development of texturized proteins using another methodology of freeze structuring. The modified methodology of Consolacion & Jelen (1986) was utilized for the development of texturized protein. The ingredients PI, WG, JFF, SA, S and L were measured and taken in a beaker and homogenized to make a slurry. The resulting slurry was then subjected to controlled freezing in an aluminium container (7.0 cm × 3.3 cm) positioned centrally within an insulating Styrofoam block (17 cm × 17 cm × 10 cm). This arrangement allowed thermal exchange only through the upper surface of the container. This directional freezing methodology was adapted to ensure unidirectional heat transfer during the solidification process. The prepared samples underwent a controlled freezing protocol designed to establish optimal structural integrity for protein analysis. Initially, the samples were maintained at -20 °C for 24 h to initiate the freezing process, followed by an extended holding period of 48 h at the same temperature to ensure complete crystallization and structural stabilization throughout the protein matrix. After the freezing phase was completed, the samples were subjected to post-processing treatment

involving thermal setting through autoclaving at 121 °C under 1.034 bar pressure for 15 min, which served to further stabilize the protein structure. The autoclaved samples were then allowed to cool to ambient temperature under controlled conditions to prevent thermal shock and structural damage. Finally, the processed samples were stored under appropriate conditions for subsequent analysis. **Figure 4.2** provides a visual overview of all sequential steps involved in the freeze structuring of protein samples. The protein structuring process began with high pressure homogenization to break down and mix protein materials. The homogenized mixture was then poured into aluminium dishes and frozen at -20 °C to set the initial structure. The frozen samples undergo heat setting through autoclaving, which used high temperature and pressure to further modify the protein structure and create a more stable matrix. Finally, the processed samples were frozen again to preserve the newly formed structured protein, resulting in a firm, gel-like product with altered texture and functional properties compared to the original protein material.

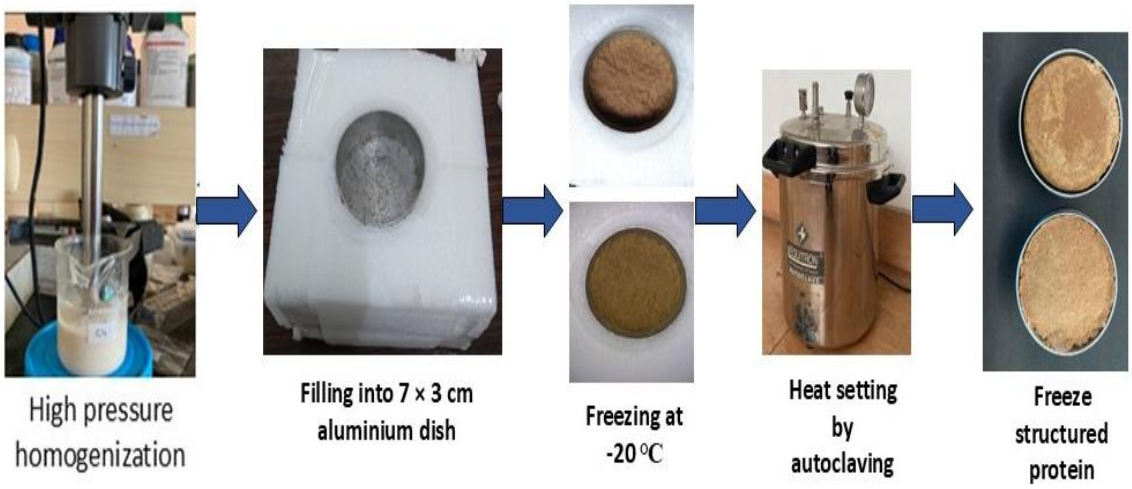

Figure 4.2: An overview of step-by-step processes involved in preparation of freeze structured protein

4.2.10. Proximate composition analysis of raw materials and texturized protein

The approximate compositions of the raw materials and texturized protein were analyzed using the AOAC (2006) standard method. The moisture content was calculated by employing a hot-air oven to dry the samples at 105 °C for 5 h. The standard Kjeldahl method using a nitrogen analyzer (N×6.25) was used to determine the protein content.

Using a Fiber Analyzer, the crude fiber concentration was measured by treating a 0.5 g sample with H_2SO_4 and NaOH. The crude fiber content was determined using the weight difference that resulted after ashing the charred samples (6 h at 550±15 °C).

4.2.11. Texture profile analysis of texturized protein

Texture profile analysis (TPA) of the samples was performed using a Texture analyzer (TAXT Plus, Stable Micro Systems, UK) through the methodology of Chiang et al. (2019) with a few modifications. The samples were cut evenly into 1×1×1 cm sizes and then compressed axially using a flat pressure adaptor with a diameter of 25 mm. The samples were subsequently compressed in two cycles with a load cell of 30 kg using a P/50 probe to 50% of their initial thickness at a crosshead speed of 60 mm/min. Hardness and springiness were the parameters that were determined from the results.

4.2.12. Analysis of colour parameters

The external colour coordinates were measured using a digital colorimeter. The device was calibrated using a typical white ceramic plate, and values for lightness (L^*), redness (a^*), and yellowness (b^*) were noted. Three randomized colour index measurements were made from various points on the sample. The mean value from three distinct locations within each sample group was employed for the statistical analysis purpose (Dutta & Sit, 2023).

4.2.13. Characterization of the optimized formulation

4.2.13.1. Determination of total phenolic content (TPC), total flavonoid content (TFC) and DPPH free radical scavenging activity

4.2.13.2. Sample extraction for TPC, TFC and DPPH free radical scavenging activity

The methanolic extraction protocol employed represents a standardized and optimized methodology for recovering bioactive compounds from texturized protein samples, utilizing 80% methanol as the extraction solvent due to its superior polarity balance that efficiently solubilizes both hydrophilic and lipophilic phenolic compounds while maintaining compound stability. The extraction conditions of 500 rpm agitation for 2 h at ambient temperature ensure maximum mass transfer and compound liberation from the

protein matrix without thermal degradation of heat-sensitive antioxidants, while the 1:10 sample-to-solvent ratio provides adequate dilution for complete extraction without excessive solvent consumption. The subsequent centrifugation at 7500×g for 15 min at 20 °C effectively separates the phenolic-rich supernatant from insoluble protein and fiber residues, yielding a clear extract suitable for spectrophotometric analysis of total phenolic content (TPC), total flavonoid content (TFC), and DPPH free radical scavenging activity without interference from particulate matter. This extraction methodology is critical for obtaining reproducible and quantitative results in antioxidant assessment, as incomplete extraction would underestimate the bioactive potential while harsh conditions could degrade the target compounds, making this optimized protocol essential for accurate characterization of the texturized protein's functional properties.

4.2.13.3. Total phenolic content (TPC)

The total phenolic content (TPC) of the sample was determined using a modified Folin–Ciocalteu assay, with gallic acid as the standard. A 20 µL aliquot of supernatant extract was mixed with 1.58 mL of distilled water and 100 µL of Folin–Ciocalteu reagent. After allowing the mixture to react for 8 min, 300 µL of 20% sodium carbonate was added. The samples were immediately vortexed and incubated in the dark at room temperature for 2 h. Absorbance was then measured at 765 nm using a UV-Vis spectrophotometer (Skanit, Thermo-Fisher Scientific). All samples and standards were analyzed in triplicate, with TPC expressed as mg of gallic acid equivalent (mg GAE) per gram of dry sample weight (Palanisamy et al., 2019).

4.2.13.4. Total flavonoid content (TFC)

The total flavonoid content (TFC) was measured following the method outlined by Palanisamy et al. (2019) with some modifications, using quercetin as the standard. A 0.25 mL aliquot of 80% methanolic extract was mixed with 1.25 mL of distilled water and 75 µL of 5% $NaNO_2$ solution. The mixture was left at room temperature for 6 min. Then, 150 µL of 10% $AlCl_3 \times 6H_2O$ solution was added, and the mixture was allowed to rest for another 5 min. Afterward, 0.5 mL of 1 M NaOH was added and thoroughly mixed. Absorbance was then measured at 510 nm using a UV-Vis spectrophotometer (Skanit, Thermo-Fisher Scientific). All samples and standards were analyzed in triplicate, and TFC was expressed as mg of quercetin equivalent (QE) per gram of dry

sample weight.

4.2.13.5. DPPH (2,2-diphenyl-1-picryl-hydrazyl) free radical scavenging activity

With some modifications, the DPPH free radical scavenging activity was determined using the methodology of Abdullah et al. (2022). The extract (3 mL) was incubated with a methanolic solution of 0.1 mM DPPH (1 mL) for 30 min in dark along with 3 mL of methanol as blank. Then absorbance of both the solutions (extract and blank) was measured using a UV-Vis spectrophotometer (Skanit, Thermo-Fisher Scientific) at 517 nm and the results (absorbance) were expressed as the percentage of inhibition (discoloration degree) of free radical of sample by DPPH against the blank (Abdullah et al., 2022).

DPPH scavenging activity was calculated according to the following formula:

$$\text{DPPH scavenging activity (\%)} = \frac{\text{Abs}_{\text{DPPH}} - \text{Abs}_{\text{sample}}}{\text{Abs}_{\text{DPPH}}} \times 100 \quad (4.1)$$

4.2.14. Visible appearance

The visual appearance of the texturized protein was assessed by following the protocol of Wi et al. (2020). Photographs of both the exterior and the interior of the samples were taken using a digital camera, and various features were distinguished.

4.2.15. Cutting force

The cutting force of the texturized protein was analyzed using a texture analyzer (TA XT Plus, Stable Micro Systems, UK) through the methodology of Chiang et al. (2019) with modifications. The sample was cut into desired shape and dimension (20×20×10 mm) using a kitchen knife. After that, a craft knife blade probe was used to cut the sample to 75% of its original thickness at a speed of 1 mm/s along the direction vertical (lengthwise strength, F_V) and parallel (crosswise strength, F_L) to the direction of fiber length, respectively. The degree of texturization (DT) was used to indicate fibrous structure formation and was expressed as the ratio of F_L and F_V.

$$\text{Degree of texturization (DT)} = \frac{F_L}{F_V} \quad (4.2)$$

4.2.16. Cooking yield and cooking loss

The texturized Samples were sliced into 2 x 2 cm (L × W) cubes and cooked in water at 80 °C for 20 min. The cooking yield was computed by measuring the mass of the samples both before and after cooking using equation (4.3) (Palanisamy et al., 2019).

$$\text{Cooking yield (\%)} = \frac{\text{Mass of cooked sample}}{\text{Mass of raw sample}} \times 100 \quad (4.3)$$

Cooking loss was calculated by using the given equation (4.4):

$$\text{Cooking loss (\%)} = (100 - \%\ \text{Cooking yield}) \quad (4.4)$$

4.2.17. Expressible moisture

The modified procedure of Palanisamy et al. (2019) was used to analyze the expressible moisture. One gram of cooked, texturized protein was sandwiched between two filter sheets and compressed using a hand press that weighed around ten kilograms. Pressure was applied to the sample for two min. Expressible moisture was represented as a percentage of the net mass change from the beginning mass after the mass of the sample was measured both before and after the pressing process (equation 4.5).

$$\text{Expressible moisture (\%)} = \frac{(\text{Initial mass} - \text{Squeezed mass})}{\text{Initial mass}} \times 100 \quad (4.5)$$

4.2.18. *In-vitro* protein digestibility (IVPD)

The *in-vitro* protein digestibility was determined using the modified methodology of Hsu et al. (1977) and Flores-Jiménez et al. (2022). 10 mL of aqueous protein suspension (312.5 mg protein) was prepared in distilled water and adjusted to pH 8.0 with 0.l M HCl and/or NaOH while stirring at 37 °C. The multienzyme solution was prepared (2.5 mg trypsin, and 50 mg pancreatin/50 mL) in distilled water and refrigerated till further use. 7.5 mL of the multienzyme solution were then added to the protein suspension which was being stirred at 37 °C. The pH began to drop instantly. A pH meter was used to automatically record the pH reduction during a 10 min period. The IVPD was further calculated using the given equation (4.6):

$$\text{IVPD (\%)} = [210.464 - 18.103(X_1)] \quad (4.6)$$

Where, X_1 = pH at 10 min.

4.2.19. Morphology using Scanning electron microscopy (SEM)

With minor adjustments, the methodology of Samard & Ryu (2019) was used to analyze the microstructure of the texturized protein. The samples were cut into 3 mm width and 10 mm length pieces, and subjected to immediate freezing with liquid nitrogen slush, and then broken. Using an Emitech K1250 Cryo-SEM equipment, free water was extracted from the samples at -8 ℃ for 4 h while they were under vacuum at 1×10^{-4} mbar. After that, gold was sputter coated on the sample surfaces, and pictures were captured by Cryo- SEM (JEOL JSM- 6460 LV, Japan) at -180 ℃.

4.2.20. Comparison of the properties of texturized proteins developed from two texturization methods

Different protein texturization methods, namely freeze texturization and freeze structuring, were employed to develop meat analogues using protein-based formulations, with a commercial texturized soy protein sample included as a reference. The visual appearance of samples was evaluated through surface and cross-sectional imaging to assess fiber formation, compactness, and textural orientation. The physicochemical and functional properties of the texturized proteins were analysed by measuring moisture content, protein content, cooking yield, expressible moisture, and color parameters (L^*, a^*, b^*). The textural characteristics were also assessed using a texture profile analyser to determine hardness, springiness, cohesiveness, resilience, adhesiveness, gumminess, and chewiness, while also measuring cutting forces in both vertical and parallel directions to calculate the degree of texturization indicating anisotropy in the fibrous structure. The results were then compared among methods to determine the most effective technique for achieving desirable structural and functional properties in plant-based meat analogues.

4.2.21. Statistical analysis

The statistical analysis of experimental data was conducted using SPSS statistical software (IMS SPSS Statistics 26), where the means of triplicate experimental values were systematically calculated to ensure data reliability and reduce experimental error. To determine statistical significance among treatment groups, one-way analysis of variance (ANOVA) was employed as the primary statistical test to evaluate whether

observed differences between groups were statistically meaningful rather than due to random variation. Following the ANOVA analysis, Duncan's multiple range test was applied as a post-hoc comparison procedure to identify specific group differences and establish homogeneous subsets among the treatment means. The statistical significance threshold was established at a probability level of $p<0.05$, meaning that differences with less than 5% probability of occurring by chance alone were considered statistically significant.

4.3.Results and discussion

4.3.1. Proximate composition analysis of raw materials

The proximate composition of Manila tamarind seed protein isolates (MTSPI) is presented in **Table 4.3**. The moisture content of the isolates was 4.8%. The MTSPI have an 85.17% protein content. Native chickpea protein isolates (85.78 and 85.08 g/100 g) (Sofi et al., 2020), orange seed protein isolates (86.38%) (Rosas et al., 2022) including Indian black gram protein isolates (*Vigna mungo* L.) varieties (Wani et al., 2015a) all showed comparable protein contents (81.0 to 86.3%).

Table 4.3: Proximate composition of Manila tamarind seed protein isolate (MTSPI) and jackfruit flour

S. No.	Parameters	Sample values	
		MTSPI	**JFF**
1	Moisture (%)	4.8 ± 0.11	9.4 ± 0.13
2	Carbohydrates (%)	4.97 ± 0.08	79.7 ± 2.01
3	Crude fiber (%)	-	8.82 ± 0.18
4	Protein (%= N × 6.25)	85.17 ± 0.31	4.36 ± 0.02
5	Total ash (%)	4.28 ± 0.14	5.76 ± 0.16

Values are expressed as the average of triplicates ± standard deviation (MTSPI: Manila tamarind seed protein isolate; JFF: Jackfruit flour)

The proximate composition analysis of protein isolates and jackfruit flour reveals critical nutritional parameters that significantly ($p<0.05$) influence their functional and commercial viability. The protein content variations observed in isolates, as highlighted by Nunes et al. (2017), demonstrate the multifactorial nature of protein extraction

efficiency, where the initial cultivar protein content serves as the foundation, while protein composition heterogeneity and extraction methodology optimization determine the final yield and quality. These parameters are crucial because they directly impact the Manila tamarind seed protein isolate's nutritional density, functional properties such as emulsification and gelation, and ultimately the cost-effectiveness of the extraction process. The ash content of 4.28% in the isolates indicated substantial mineral retention, closely aligning with the values for kidney bean protein isolates (4.32-4.57%) reported by Wani et al. (2015b), suggesting comparable mineral bioavailability and nutritional supplementation potential. The jackfruit flour's moisture content of 9.4% represents an optimal balance for storage stability and processing functionality, as values below 10% typically prevent microbial proliferation while maintaining powder flowability characteristics. The crude protein content of 4.36% in jackfruit flour, corroborated by Feili et al. (2013) findings of 4.52%, establishes this flour as a moderate protein contributor suitable for nutritional fortification applications. However, the crude fiber content value reported in the current study (8.82%) and was somewhat lower than that of Feili et al. (2013) observations (11.32%), and highlights few critical analytical challenges in fiber quantification. This reduction likely stems from incomplete enzymatic hydrolysis during fiber isolation, interference from lignin or resistant starch components, or inherent sample variability due to fruit maturity differences (Feili et al., 2013). These proximate parameter variations are industrially significant as they affect product standardization, nutritional labelling accuracy, and functional ingredient performance in food formulations.

4.3.2. Experimental modelling of mixture design

The comprehensive analysis of variance (ANOVA) analysis presented in **Table 4.4** demonstrates exceptional model reliability through multiple statistical validation parameters, with coefficient of determination (R^2) values ranging from 0.9653 to 0.9990, indicating that the quadratic models explain 96.53% to 99.90% of the total variation in hardness, springiness, fiber, and protein responses. The R^2 values obtained for all response variables demonstrated exceptional proximity to unity, indicating that the developed quadratic polynomial models exhibited minimal unexplained variance and possessed robust predictive capabilities for accurately forecasting the experimental outcomes. The statistical validation was further reinforced by non-significant lack of fit

($p>0.05$) test results across all four measured responses, which conclusively confirmed the adequacy of the model framework and verified that the quadratic polynomial equations successfully captured the complex relationships between the independent processing variables and their corresponding responses without any systematic deviations or bias. These statistical measures collectively demonstrated that the models were well-fitted to the experimental data and could reliably predict response behavior within the studied parameter space. The comprehensive contour plots presented in **Figure 4.3** provided intuitive visual representations of the response surfaces, effectively illustrating the interactive effects of processing parameters on the measured outcomes. These graphical tools served as valuable optimization aids, enabling researchers to identify optimal processing parameter combinations that would achieve the desired textural properties and nutritional characteristics in the final product while minimizing processing costs and maximizing product quality.

Table 4.4 presents a comprehensive ANOVA analysis that serves as definitive statistical validation for the quadratic model's exceptional predictive performance across four critical quality parameters through systematic and rigorous statistical evaluation procedures. The model terms governing hardness, springiness, fiber content, and protein content consistently demonstrated highly significant relationships with p-values less than 0.0001, indicating extremely strong statistical significance. The coefficient of determination (R^2) values of 0.9653, 0.9791, 0.9950, and 0.9927 represent outstanding model fit quality, effectively explaining 96.53%, 97.91%, 99.50%, and 99.27% of the total experimental variation respectively. The detailed examination of interaction term significance patterns revealed complex and sophisticated processing dynamics underlying the experimental system, where specific two-factor interactions including AB, BC, BD, BE, and BF consistently demonstrated statistical significance ($p<0.05$) across multiple response variables. This consistent significance pattern strongly suggests that these particular parameter combinations exhibit either synergistic enhancement or antagonistic inhibition effects that cannot be accurately predicted or understood through simple additive consideration of individual factor effects alone. The presence of these interaction effects underscores the multivariate complexity inherent in food processing systems and validates the necessity of employing response surface methodology for comprehensive process optimization.

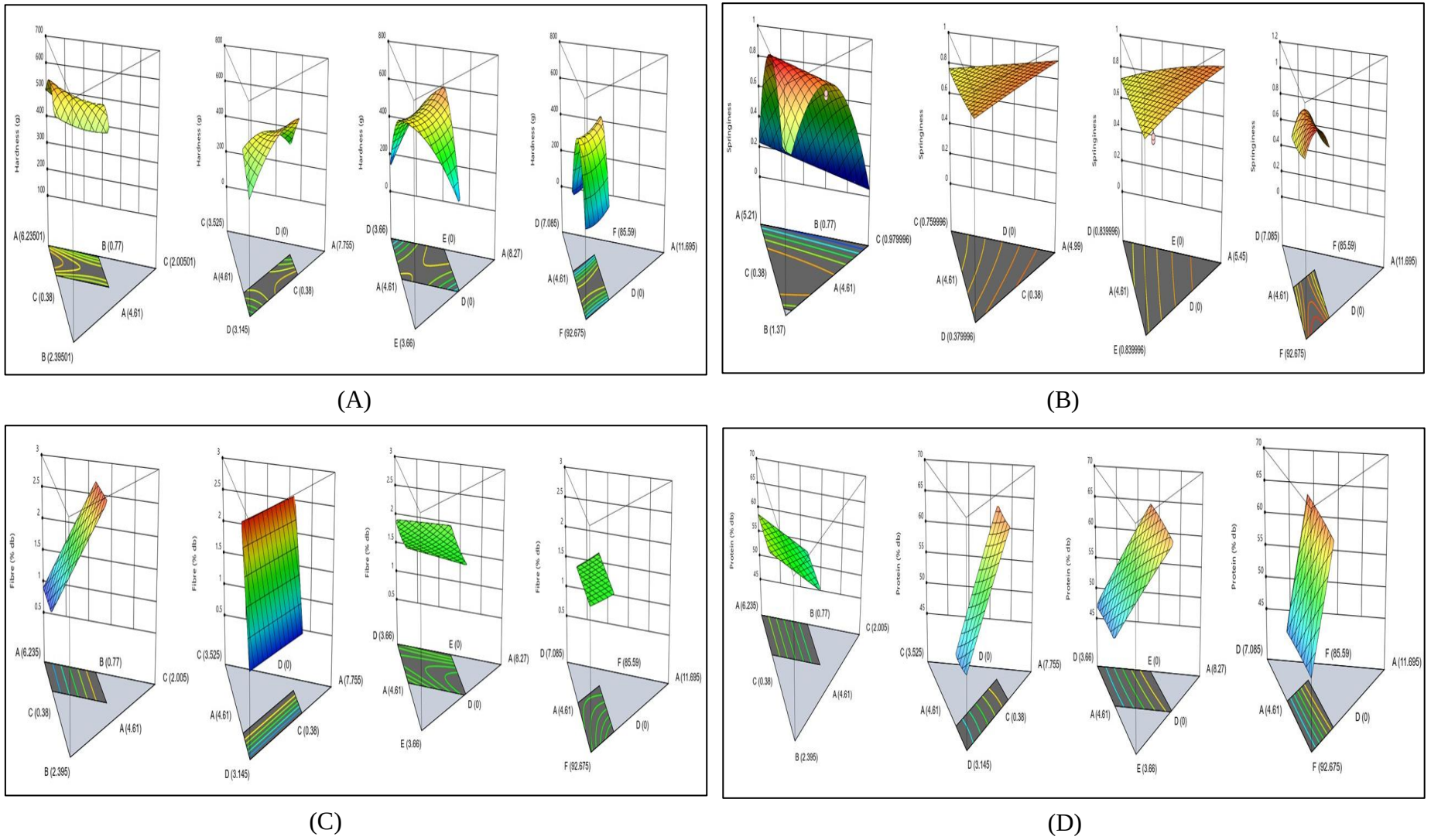

Figure 4.3. 3D surface plot of (A) Hardness, (B) Springiness, (C) Fibre content, and (D) Protein content of texturized protein

Table 4.4: ANOVA table for the quadratic model

Terms	**Responses**							
	Hardness		**Springiness**		**Fiber content**		**Protein content**	
	Sum of Squares	**p-value**	**Sum of Squares**	**p-value**	**Sum of Squares**	**p-value**	**Sum of Squares**	**p-value**
Model	7.87×10^{5}	< 0.0001*	1.92	< 0.0001*	17.30	< 0.0001*	1597.09	< 0.0001*
Quadratic	73104.36	0.0134*	0.2944	0.0003*	17.30	< 0.0001*	1578.76	< 0.0001*
AB	19831.32	0.0245*	1.08	< 0.0001*	0.0392	0.0009*	0.1962	0.0069*
AC	1323.00	0.5100	0.0000	0.9303	0.0068	0.0803	2.87	< 0.0001*
AD	25468.48	0.0134*	0.0715	0.0019*	0.0000	0.9383	2.75	< 0.0001*
AE	3060.39	0.3233	0.0154	0.0817	0.0132	0.0217*	2.81	< 0.0001*
AF	2143.78	0.4049	0.0894	0.0009*	0.0002	0.7434	2.79	< 0.0001*
BC	15525.34	0.0413*	0.7545	< 0.0001*	0.0516	0.0003*	1.11	0.0001*
BD	28031.28	0.0104*	0.9375	< 0.0001*	0.0402	0.0008*	0.0230	0.1906
BE	24855.68	0.0143*	1.04	< 0.0001*	0.0365	0.0011*	0.3998	0.0015*
BF	24149.90	0.0153*	1.02	< 0.0001*	0.0404	0.0008*	0.8782	0.0002*
CD	250.16	0.7725	0.0233	0.0387*	0.0065	0.0864	1.85	< 0.0001*
CE	364.61	0.7273	0.0240	0.0364*	0.0024	0.2758	2.32	< 0.0001*
CF	762.46	0.6153	0.0168	0.0705	0.0052	0.1185	0.1086	0.0218*
DE	22496.60	0.0183*	0.0002	0.8195	0.0119	0.0278*	2.06	< 0.0001*
DF	5.74×10^{5}	< 0.0001*	0.0031	0.4050	5.26×10^{-6}	0.9579	0.3715	0.0017*
EF	610.21	0.6526	0.0000	0.9259	0.0134	0.0212*	1.44	< 0.0001*
R-Squared	0.9653		0.9791		0.9950		0.9927	
Lack of Fit	11989.29	0.6293	0.0299	0.1538	0.0861	0.4172	1.34	0.3790

Values in asterisk (*) are significant terms

Particularly noteworthy throughout the analysis is the consistent statistical significance of quadratic terms across all measured responses, providing definitive confirmation of non-linear relationships between processing parameters and product quality attributes. This quadratic significance conclusively justifies the selection and implementation of second-order polynomial models rather than relying on simpler linear approximations that would inadequately capture the true nature of these complex relationships. Most critically important for model validation purposes, the non-significant lack of fit test results, with respective p-values of 0.6293, 0.1538, 0.4172, and 0.3790, provide conclusive confirmation of model adequacy by demonstrating that the fitted polynomial equations successfully capture the true underlying mechanistic relationships without introducing systematic deviations or bias, thereby validating their reliable application for process optimization, predictive modeling, and quality control in food product development and manufacturing applications.

4.3.3. Effect of freezing on structure formation

The ice crystallization structures were visually examined to assess the effects of freezing and stabilization processes **(Figure 4.4)**. In the initial freezing phase, the material formed a gel-like structure as it solidified. This structure was then further stabilized by treatment with calcium chloride ($CaCl_2$), which played a key role in maintaining the integrity of the gel. However, during the second freezing stage, the ice crystals generated caused some distortion to the pre-formed gel structure (Teng & Campanella, 2023). Interestingly, after the first freezing stage, the structures across all samples showed minimal differences, suggesting that the initial frozen structures were effectively stabilized by the $CaCl_2$ treatment. The stabilizing effect is attributed to the formation of calcium alginate, which acts as a robust gel network, particularly when sodium alginate is present (Lee & Hong, 2020). This combination enhances the gel's stability by creating stronger cross-linking. The carbohydrate polymers, like alginate, can bind water molecules effectively due to their polyol structures (containing hydroxyl groups) and negatively charged groups such as sulphur and carboxyl groups (Chen et al., 2023). These groups engage in hydrogen bonding and ion-dipole interactions, thereby reinforcing the gel matrix and improving the structural integrity of the frozen material during the subsequent freezing processes (Sha & Siong, 2020).

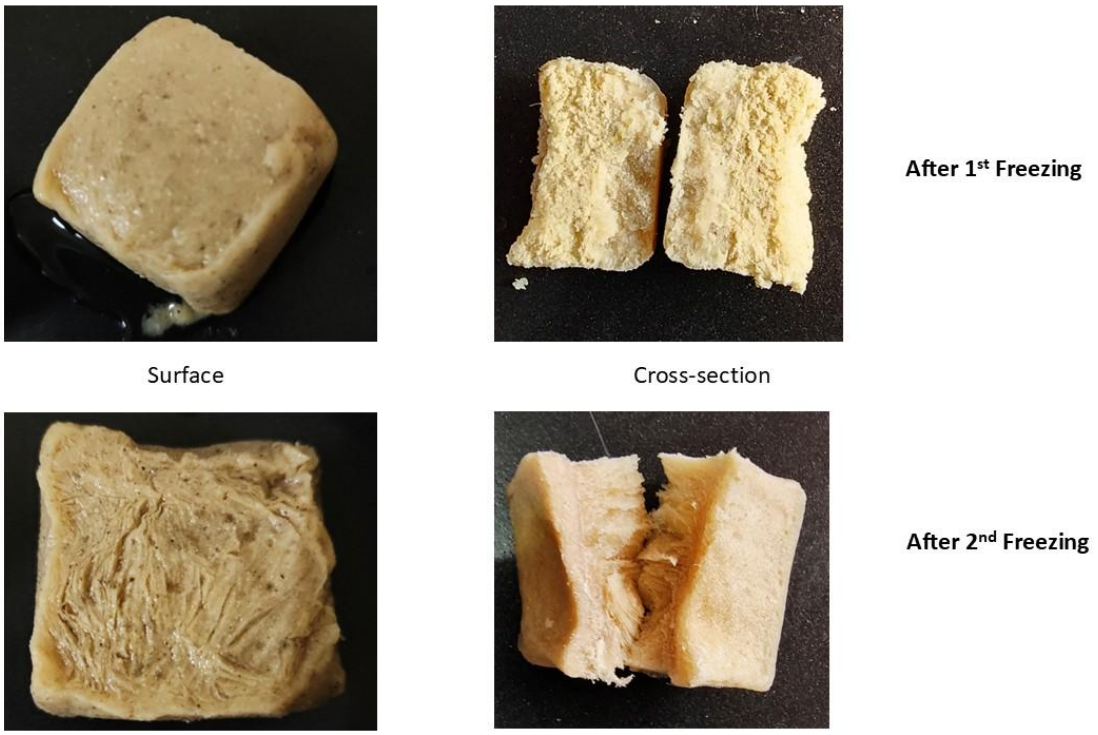

Figure 4.4: Visual appearance of the texturized protein prepared through freeze texturization process

This increases the thickness and product consistency and decreases water loss during cooking. Some cooked meat analogues have a delicate texture that can be attributed to polysaccharides. Because aqueous calcium alginate tends to form a gel that solidifies quickly, it is used to attach onto specific items.

4.3.4. Colour properties of texturized protein

The colour values of the texturized Manila tamarind seed protein are shown in **Table 4.5**. The *L** value of the texturized protein varied only slightly with the changes in values of its different constituents and ranged from 55.33 to 69.08. It was observed that texturized protein with higher PI, WG and L component values had most lightness compared to the samples with lower protein isolate (PI), wheat gluten (WG), liquid (L, consisting of oil and water) and higher sodium alginate (SA) contents.

The same outcomes were observed by Chiang et al. (2019) during their research on the impact of soy protein to wheat gluten ratio upon physicochemical qualities of extruded meat analogues. They reported the *L** values of the extruded meat analogues in the range of 58.01 to 61.44. Cooked chicken breast had higher *L** values (77.16) compared with meat analogues due to its distinct composition having higher fat content and lower carbohydrate composition. The *a** value of the texturized protein ranged from 3.42 to 9.52. The change in the *a** value from 3.42 to 9.52 indicates a significant shift towards greater redness in the colour of the product, demonstrating enhanced chromatic properties that bring the texturized protein visually closer to authentic meat appearance. This substantial increase in redness suggested that the processing conditions, ingredient modifications, or additive incorporation successfully enhanced the red coloration that is characteristic of conventional meat products, where higher *a** values directly correlate with consumer perception of meat-like quality and freshness (Zhou et al., 2022). Comparable results were reported by Lee et al. (2022) for extruded meat analogues with their *a** values ranging from 6.46 to 8.41, confirming that similar chromatic improvements can be achieved through various plant-based formulation strategies and processing techniques. The *b** values of the texturized protein ranged from 18.05 to 29.67, indicating varying degrees of yellowness that contribute to the overall color complexity and visual appeal of the final product. These results were in agreement with the findings of Lee et al. (2022), as the *b** values of their extruded meat analogues ranged from 16.76 to 23.90, suggesting consistent color development patterns across different plant-based formulations and processing methods. Similarly, Zhou et al. (2022) reported *b** values of 16.3 for plant-based burgers, further validating the color range typically observed in commercially viable meat alternatives. For comparison, the *a** and *b** values of cooked chicken breast were found to be 3.29 and 13.13 respectively, providing a benchmark against which the texturized protein's color development can be evaluated (Kumar et al., 2021).

These color measurements prove that strategic formulation and processing can effectively bridge the visual gap between plant-based alternatives and traditional meat products, addressing one of the primary barriers to consumer adoption in the alternative protein market (Lee et al., 2022).

Table 4.5: *L**, *a** and *b** values of the different runs of the experimental design

Run	A:PI	B:WG	C:JFF	D:SA	E:S	F:L	Colour		
Units	%	%	%	%	%	%	*L**	*a**	*b**
1	6.53	0.9	1.15	3.6	1.8	86.02	58.05	5.83	20.77
2	6.4	1.33	0.56	2.62	1.8	87.29	62.71	6.07	22.69
3	4.78	1.33	1.15	3.6	1.8	87.34	55.33	6.79	21.44
4	6.53	1.33	1.15	1.13	1.8	88.06	58.25	4.8	18.05
5	5.24	1.13	0.38	3.6	1.54	88.11	67.08	8.22	28.53
6	6.53	1.33	0.38	3.6	0	88.16	65.05	9.52	29.67
7	5.89	0.77	0.78	3.6	0.72	88.24	59.22	7.03	24
8	6.22	1.27	1.15	2.21	0.58	88.57	63.57	6.47	26.53
9	6.22	1.27	1.15	2.21	0.58	88.57	64.76	8	27.97
10	5.48	1.33	0.77	1.53	1.79	89.1	67.11	6.83	28.11
11	4.61	0.77	0.76	2.73	1.8	89.33	55.56	6.37	18.94
12	6.53	0.98	0.38	1.74	0.85	89.52	60.97	5.23	19.35
13	6.53	0.98	0.38	1.74	0.85	89.52	66.46	6	23.82
14	6.53	1.14	0.92	0	1.8	89.61	66.51	5.45	26.6
15	6.05	0.77	0.38	3.13	0	89.67	64.26	6.58	23.51
16	4.61	0.96	1.15	3.6	0	89.68	57.25	6.98	21.74
17	5.35	0.83	1.15	0.91	1.41	90.35	64.24	8.69	27.23
18	5.35	0.83	1.15	0.91	1.41	90.35	64.32	6.46	28.72
19	4.61	1.33	0.61	2.54	0.45	90.46	64.3	7.24	28.83
20	5.68	1.02	0.71	1.92	0	90.67	59.58	8.43	28.14
21	5.68	1.02	0.71	1.92	0	90.67	63.7	6.93	28.15
22	5.92	0.77	0.38	0	1.8	91.13	64.19	7.36	28.85
23	4.61	1.33	0.38	0.35	1.8	91.53	66.85	4.57	23.62
24	6.53	0.77	1.15	0	0	91.55	65.14	5.72	26.18
25	4.61	0.77	0.38	2.52	0	91.72	66.61	7.93	29.58
26	4.61	1.33	1.15	1.17	0	91.74	62.68	7.22	27.72
27	5.89	1.33	0.38	0	0.17	92.23	69.08	3.42	20.21
28	4.69	0.99	0.68	0	0.76	92.88	63.55	3.97	21.21
29	4.69	0.99	0.68	0	0.76	92.88	64.47	8.4	24.47
30	4.61	1.33	1.15	0	0	92.91	63.96	6.52	28.35
31	4.61	0.77	0.38	0	0	94.24	62.61	4.71	24.02

PI: Manila tamarind seed protein isolate; WG: wheat gluten, JFF: raw jackfruit flour; SA: sodium alginate; and S: common salt; L: liquid phase consisting of sunflower oil and water in 1:10

The comprehensive color profile achieved through these modifications represents a significant advancement in creating visually authentic plant-based meat alternatives that can compete effectively with conventional products in terms of consumer perception and market acceptance.

4.3.4. Hardness of the texturized protein

Hardness is defined as the highest force applied during the first compression. The contour plot **(Figure 4.3 A)** reveals that when PI (Protein Isolate) is at its highest value of 6.23%, hardness reaches its peak at around 550 g, particularly when WG (Wheat Gluten) is relatively low (around 0.38%) and JFF (Jackfruit Flour) is moderate (around 0.77%). As PI decreases, with WG increasing towards its maximum of 2.39% and JFF reaching around 2.00%, hardness drops to around 450 g. Intermediate combinations, where PI is around 4.61%, WG around 1.5-2%, and JFF near 1%, result in hardness levels of about 500 g. These numerical trends suggest that PI is the most significant contributor to increasing hardness, while higher levels of WG and JFF reduce overall hardness. PI, JFF, sodium alginate (SA), and liquid (L) individually increased hardness, with JFF showing the strongest effect. WG alone decreased hardness but increased it when combined with SA, JFF, F, and L, indicating WG should be used in combination to achieve desired hardness. Lin et al. (2022) reported that the addition of wheat gluten did not result in any significant difference in textured-wheat-protein (TWP)-based meat analogues. Similarly, Yuliarti et al. (2021) found that incorporating wheat protein into the formulation decreased the efficacy of the freeze structuring technique for meat analogues made from plant-based derived composites. When used singularly, JFF displayed a significant positive effect on hardness, with the additional benefit of enhanced hardness when combined with SA. Pare (2019) studied the application of jackfruit flour in meat analogues, determining that the optimal formulation for developing these analogues involved a combination of defatted soy flour and raw jackfruit flour extracts. The texturized protein blend achieved desirable properties, with jackfruit flour positively affecting hardness up to a certain concentration due to fiber disruption of protein cross-linking. Sodium alginate, though negative when used alone, showed improved effects when combined with S and L. It plays a crucial role in structuring texturized protein by enhancing fiber quality, elasticity, biopolymer interactions, and controlling protein aggregate size (Lee & Hong, 2020). Salt (S) and

liquid (L) individually increased hardness without needing combination. Higher salt content created a more porous structure, improving water-binding capacity but reducing structural viscosity and spinnability. While this enhanced water-holding capacity, it also decreased mechanical properties. Salt facilitated protein self-aggregation, contributing to these effects (Cui et al., 2023). The **Figure 4.3 A** represents contour plot describing the correlation response of various components on hardness. The differences may be explained by the specific composition of the proteins and the techniques used in their preparation. The inclusion of various proteins notably influenced and resulted in diversity in the texture profile of the analogues. The textural attributes observed in this investigation could be linked to the distinct structure of the protein gel networks formed, aligning with the observations made on rheological behaviours resulting from various protein pairings (Yuliarti et al., 2021). Below is the equation (4.7) for hardness (g):

1,954.08 X1 -71,055.7 X2 + 4,868.86 X3 -4,843.08 X4 + 925.853 X5 + 146.525 X6 + 71,387.2 X1X2 -8,574.87 X1X3 + 6,792.86 X1X4 - 4,155 X1X5 -1,824.73 X1X6 + 72,564.8 X2X3 + 83,560 × X2X4 + 76,433.7 × X2X5 + 77,418.9 × X2X6 + 3,789.74 × X3X4 + -4,745.7 × X3X5 + -6,466.01 × X3X6 + 7,396.36 × X4X5 + 8,310.26 × X4X6 + -1,187.64 × X5X6 (4.7)

Where, X1 is Protein Isolate (PI), X2 is wheat gluten (WG), X3 is Jackfruit flour (JFF), X4 is sodium alginate (SA), X5 is salt (S), and X6 is liquid (L).

4.3.5. Springiness of the texturized protein

Springiness in Texture Profile Analysis (TPA) is the height at which the food rebounds during the interval between the end of the first bite and the beginning of the second. High springiness takes greater mastication energy in the mouth. The contour plot **(Figure 4.3 B)** shows springiness values from 0.2 to 0.8 based on component proportions. Highest springiness (0.8) occurred with high WG and PI, and low JFF. Springiness decreased sharply (to 0.2) as JFF increased. Mid-range values (0.4-0.6) resulted from balanced component contributions. Springiness was maximized when PI and WG compositions were high, and decreased as the value of right-side component (JFF) increased. SA and S demonstrated gradual increases initially, followed by reductions towards the end. F:L uniquely started at its highest value, decreased, increased mid-range, then declined again. Most components displayed an overall pattern of increasing springiness to a peak

(typically mid-range) before decreasing, with slight variations in the specific progression for each component. Research indicates that protein isolates, such as soy protein isolate, can influence the freeze structuring process by promoting ice crystal formation and enhancing fibrous structure formations (Sengar et al., 2023). Wheat gluten (WG) has excellent hydration capability, leading to uniform water dispersion and contributing to a soft, elastic texture and white color in extrudates when used in moderate amounts. The inclusion of glutenin also promotes a dense fiber structure, enhancing tensile strength. However, WG ratios above 50% increase dough viscosity, hindering melt flow during extrusion and raising torque requirements (Zhang et al., 2023). Jackfruit flour (JFF) and its mixture with sodium alginate (SA) and salt improve springiness, while SA alone or with salt and liquid further enhances it (Pare, 2019). Salt ions promote protein interactions, delaying gelation and increasing gel strength. Comparable findings were reported in the construction of a whole muscle meat analogues using soybean protein isolate and polysaccharides (Cui et al., 2024) and use of jackfruit by-product in the formation of healthy meat substitute (Hamid et al., 2020). The equation (1.8) for springiness is shown below:

$$-10.0287 \times X1 + -463.442 \times X2 + 26.9605 \times X3 + 0.990684 \times X4 + 0.546592 \times X5 + 0.140728 \times X6 + 526.893 \times X1X2 + -1.35637 \times X1X3 + 11.3843 \times X1X4 + 9.32055 \times X1X5 + 11.7837 \times X1X6 + 505.873 \times X2X3 + 483.243 \times X2X4 + 493.298 \times X2X5 + 503.321 \times X2X6 + -36.5408 \times X3X4 + -38.4857 \times X3X5 + -30.3931 \times X3X6 + 0.740907 \times X4X5 + -0.611127 \times X4X6 + 0.294069 \times X5X6 \quad (4.8)$$

Where, X1 is Protein Isolate (PI), X2 is wheat gluten (WG), X3 is Jackfruit flour (JFF), X4 is sodium alginate (SA), X5 is salt (S), and X6 is liquid (L).

4.3.6. Fiber content of the texturized protein

Crude fiber refers to the dietary fiber content found in plant-based foods, primarily derived from the cell walls of plants. Crude fiber in food plays a vital part in maintaining overall good health and wellness. Contour plots of various protein components and other ingredients as functions of fiber content (%) illustrate significant variation among different components depicted in **Figure 4.3 C**. Fiber values increased drastically for protein isolate (PI) and jackfruit flour (JFF) reaching up to 2.5%, while for wheat gluten (WG), values decreased (around 1%) with the increase in concentration. A similar trend

was observed for JFF, with values that increased with increase in concentration and reached highest value at 2.77% for JFF content of 1.15%. This indicates that increasing the content of jackfruit flour could elevate the fiber content of texturized protein. All components except wheat gluten have demonstrated positive responses to fiber content individually shown in the **Table 4.2**. From the **Table 4.2**, it shows that the addition of wheat gluten led to a decrease in fiber content. As a result, it may lead to decrease in water and oil absorption that can cause poor texture and chewiness, whereas incorporating other components such as protein isolate can improve degree of hardness and chewability of the final product (Ishaq et al., 2022). Positive responses have been observed when JFF was combined with SA, S, and L. Studies have indicated that utilizing jackfruit by-products, including jackfruit flour, in the development of texturized protein can lead to a significant decrease in hardness and chewiness (Hamid et al., 2020). The soluble dietary fiber content in jackfruit not only aids in cholesterol removal from the body but also enhances the sensory and psychochemical properties of meat analogues (Pare, 2019; Yong et al., 2020). Empirical models derived from fitting responses on mixture design equations aid in studying process and response variables, along with creating 2D contour plots amongst dependent and independent variables presented in below equation (4.9):

$$\text{Fiber content (\%)} = 1.22963 \times X1 - 92.9201 \times X2 + 4.22774 \times X3 + 0.827205 \times X4 + 5.46187 \times X5 + 0.931403 \times X6 + 100.339 \times X1 \times X2 + 19.4392 \times X1 \times X3 + 0.143232 \times X1 \times X4 - 8.6446 \times X1 \times X5 - 0.562119 \times X1 \times X6 + 132.312 \times X2 \times X3 + 100.036 \times X2 \times X4 + 92.6295 \times X2 \times X5 + 100.11 \times X2 \times X6 + 19.3039 \times X3 \times X4 + 12.1401 \times X3 \times X5 + 16.941 \times X3 \times X6 + -5.37163 \times X4X5 + 0.025155 \times X4X6 - 5.56227 \times X5X6 \quad (4.9)$$

Where, X1 is Protein Isolate (PI), X2 is wheat gluten (WG), X3 is Jackfruit flour (JFF), X4 is sodium alginate (SA), X5 is salt (S), and X6 is liquid (L).

4.3.7. Protein content of the texturized protein

Composed of long chains of amino acids, proteins are involved in virtually every biological process, serving as structural components, enzymes, hormones, and immune system molecules. Adequate protein intake is essential for overall health, particularly for muscle growth, immune function, and hormone regulation. The contour plot **(Figure 4.3 D)** shows the effect of PI (Protein Isolate), WG (Wheat Gluten), and JFF (Jackfruit

Flour) on protein content of the texturized protein. With the increase in concentration of PI (from 4.61 to 6.53%), the protein content exhibited an increasing trend, with values gradually rising towards the end (66.15%). Similarly, increase in WG from 0.77 to 1.33%, a similar trend of increasing protein content (45.14 to 66.15%) values towards the end. With increase in concentration of JFF from 0.38% to 1.15%, protein content decreased with lowest value at 49.84%. The positive responses varied among the components and their combinations. Each component exhibited increased protein content when added alone, except for JFF, salt, and liquid. However, when combined with every component, they showed positive responses towards protein content, including protein isolate (PI), jackfruit flour (JFF), sodium alginate (SA), salt (S), and liquid (L), thereby imparting appropriate properties like texture, gelation, etc. to products (Sha & Xiong, 2020). The nutritional composition of jackfruit by-products in meat analogues depicted increased levels of protein and dietary fiber (Hamid et al., 2020). Protein isolate contributes to enhanced properties in meat analogues by providing better gelation properties, improving texture, and enhancing overall quality (Kurek et al., 2022). Most proteins obtained from legumes have gel-forming capabilities, which is essential for attaching particles, immobilizing fat, and entrapping water inside the matrix of emulsion-type alternative protein products (Sha & Xiong, 2020). Sodium alginate functions as a gelling agent and emulsifier, helping entrap lipids and proteins, mimicking the texture and appearance of real animal fat (Teng et al., 2023). Additionally, with the salt incorporation, protein aggregates further, showed lower structural viscosity index and improved spinnability. Zeng et al. (2023) demonstrated that mixing sodium alginate (SA) and soy protein isolates (SPI) produced a high-protein-level composite for plant-based meat analogue. As protein content enhances, salt ions move out of the composite rapidly, resulting in a more porous structure (Zeng et al., 2023). The equation (4.10) for protein content (%) is shown below:

$$126.655 \times X1 + -787.069 \times X2 + 339.717 \times X3 + 36.5904 \times X4 + 16.4765 \times X5 + 46.5533 \times X6 + 1{,}069.9 \times X1X2 + -547.981 \times X1X3 + 35.5137 \times X1X4 + -57.1663 \times X1X5 + -11.7951 \times X1X6 + 638.416 \times X2X3 + 877.306 \times X2X4 + 1{,}144.97 \times X2X5 + 826.702 \times X2X6 + -217.598 \times X3X4 + -93.6282 \times X3X5 + -282.869 \times X3X6 + -15.8363 \times X4X5 + 7.80275 \times X4X6 + 43.8722 \times X5X6 \quad (4.10)$$

Where, X1 is Protein Isolate (PI), X2 is wheat gluten (WG), X3 is Jackfruit flour (JFF),

X4 is sodium alginate (SA), X5 is salt (S), and X6 is liquid (L).

4.3.8. Validation of optimization of texturization parameters

The final phase of optimization was the validation of the optimal modifications of different constituents namely seed protein isolate (PI), wheat gluten (WG), raw jackfruit flour (JFF), sodium alginate (SA), common salt (S) and liquid (L). The response optimization tool in Design Expert software was utilized to find the optimum blend of ingredients PI, WG, JFF, SA S and L that need to be varied to develop superior product. The optimum points were determined by considering maximum PI, maximum WG, maximum JFF, maximum SA, minimum S, minimum L, minimum hardness, maximum springiness, maximum fiber content and maximum protein content.

Table 4.6: Optimized values of the different constituents along-with predicted and experimental values of the response variables

Design factors		**Optimum amount in formulation**
PI		6.53%
WG		1.23%
JFF		1.15%
SA		3.6%
S		0
L		87.48%
Responses	**Predicted values**	**Experimental values**
Hardness (g)	485.34	481.08
Springiness	0.74	0.69
Fibre (%)	2.72	2.16
Protein (% d.b.)	65.66	64.12

PI: Manila tamarind seed protein isolate; WG: wheat gluten, JFF: raw jackfruit flour; SA: sodium alginate; and S: common salt; L: liquid phase consisting of sunflower oil and water in 1:10

The optimum points were obtained as 1 for X1, 0.932 for X2, 1 for X3, 1 for X4, 0 for X5 and 0.928 for X6. The corresponding encoded values for the optimum points were calculated as 6.53% for PI (protein isolate), 1.24% for WG (wheat gluten), 1.15% for JFF (jackfruit flour), 3.6% for SA (sodium alginate) and 87.48% for L (liquid) **(Table 4.6)**. The predicted responses at the optimum points were 485.03 g for hardness, 0.74 for springiness, 2.72% for fiber content and 65.66% for protein content. The projected values for reactions were empirically validated. **Table 4.6** summarizes the optimization and verification outcomes. The predicted and experimental values were almost always comparable. The difference was in fibre content where the experimental value was a bit lower (2.16%) than the one predicted (2.72%). All other obtained values for the optimized sample were significantly similar. This finding confirms the ability of the constituents (PI, WG, JFF, SA, S, and L) to produce the desired structure of plant-based meat analogues that is comparable to that of conventional products. The most beneficial outcome was substantial similarities in the textural attributes of the product and their high protein content when compared with cooked chicken.

4.3.9. Characterization of the optimized formulation

4.3.9.1. Physicochemical characterization

4.3.9.1.1. Moisture content (M.C.)

The moisture content (M.C.) of the texturized protein was 45.93% **(Table 4.7)**, closely aligning with the reference texturized vegetable protein, which had a moisture content of 44.53%. This similarity suggests comparable water-binding capacities and structural hydration between the samples. The reference sample contained ingredients such as water, soy flour, soy isolate, whole wheat flour, wheat gluten, soya extract, salt, and an acidity regulator (INS 330), all of which contribute to moisture retention. The presence of soy components and gluten enhances water absorption and retention, supporting the observed moisture content values. This alignment indicates that the developed protein product achieves a similar hydration profile to commercially accepted alternatives. The moisture content of texturized vegetable proteins (TVPs) represents a fundamental quality control parameter that governs multiple critical aspects of product performance and commercial viability (Samard et al., 2021). The optimal moisture range of 7-10% for dried TVPs, as established in storage protocols, was scientifically significant because it falls below the critical water activity threshold (a_w<0.6) that inhibits microbial growth,

enzymatic deterioration, and Maillard browning reactions, thereby ensuring extended shelf life and food safety compliance (Ketnawa & Rawdkuen, 2023).

Table 4.7: Physicochemical and functional properties of the freeze texturized protein and reference sample

Parameters	Freeze texturized protein	Texturized soy-protein*
Moisture (%)	45.93±0.17[a]	44.53±0.36[b]
Fiber (%)	2.16±0.02[b]	4.5±0.03[a]
Fat (%)	4.03±0.08[b]	5.45±0.06[a]
Protein (%db)	64.12±0.35[a]	30.11±0.17[b]
Cooking Yield (%)	86.33±0.98[b]	90.33±0.74[a]
Cooking loss (%)	13.67±0.98[a]	9.67±0.74[b]
Expressible Moisture (%)	11.65±0.13[b]	12.05±0.05[a]
***In-vitro* protein digestibility (%)**	64.33±0.38[b]	75.61±0.26[a]
Total Phenolic Content (mg GAE/g)	1.52±0.04[a]	1.41±0.02[b]
Total Flavonoid Content (mg QE/g)	1.29±0.02[a]	0.63±0.01[b]
DPPH free radical scavenging (% inhibition)	39.83±0.16[a]	31.2±0.12[b]

Values are expressed as the average of triplicates ± SD. Different superscripts within the same row are significantly different ($p<0.05$) (* Signifies reference sample)

During extrusion processing, moisture content acts as a plasticizing agent that directly influences protein denaturation kinetics, starch gelatinization, and fiber matrix formation, with higher moisture levels (typically 25-35% during processing) facilitating protein unfolding and realignment necessary for meat-like texture development (Hong et al., 2022). The integrity index, which measures the structural stability of extruded products,

is inversely related to excessive moisture content, as water acts as a lubricant that can weaken intermolecular protein bonds and reduce fibrous structure formation essential for meat analogue applications. Conversely, the nitrogen solubility index and water absorption capacity are positively correlated with controlled moisture levels, indicating optimal protein functionality for rehydration and cooking performance (Samard et al., 2021). The interplay between temperature and moisture content creates a synergistic effect on protein texturization, where precise moisture control enables optimal thermal energy transfer for protein modification while preventing thermal degradation (Samard et al., 2021). This moisture-temperature relationship is particularly critical because deviations beyond the optimal range can result in either insufficient protein restructuring (leading to poor texture) or excessive protein denaturation (causing reduced nutritional quality and off-flavors), ultimately determining consumer acceptance and market success of plant-based meat alternatives.

4.3.9.1.2. Fiber content

The fiber content of the freeze texturized protein was 2.16% **(Table 4.7)** which was quite lower than the reference material (TVP) whose fiber content value was 4.5%. The fiber content of texturized protein products is an important consideration, as it not only contributes to the overall nutritional profile but also influences the textural properties and processing characteristics of the product (Kinsella, 2018). The fiber content of 2.16% in texturized protein represents a strategically significant compositional parameter that reflects deliberate processing optimization to balance nutritional value with textural functionality in meat analogue applications. This relatively low fiber level indicates extensive processing refinement, likely involving dehulling, milling, or protein concentration techniques that selectively remove fibrous plant cell wall components while preserving protein functionality, which is critical for achieving the smooth, cohesive texture consumers expect in meat substitutes (Kinsella, 2018). From a nutritional perspective, this reduced fiber content represents a trade-off between textural quality and the established health benefits of dietary fiber, including improved digestive health, cholesterol reduction, and glycemic control, suggesting that manufacturers prioritize sensory acceptance over maximum nutritional density (Anjum et al., 2011). The significance of this parameter becomes evident when compared to typical TVP compositions, where fiber contents often range from 5-15%, indicating that this

particular formulation has undergone more intensive processing to achieve superior textural properties (Arueya et al., 2017). Texturally, the low fiber content is functionally advantageous because excessive dietary fiber can create undesirable grittiness, heterogeneous mouthfeel, and structural discontinuities that compromise the meat-like eating experience, while the 2.16% level provides sufficient structure for binding without interfering with protein gel formation during cooking (Chen et al., 2023). This fiber level also impacts water-holding capacity and cooking behaviour, as lower fiber content typically correlates with improved protein hydration, more uniform heat transfer, and enhanced protein-protein interactions that are essential for developing the elastic, chewy texture characteristic of quality meat analogues (Arueya et al., 2017). The commercial significance of this parameter lies in its influence on consumer acceptance, as products with optimized fiber levels demonstrate better sensory scores and market performance compared to high-fiber alternatives that may satisfy nutritional guidelines but fail to meet textural expectations in the competitive plant-based protein market.

4.3.9.1.3. Fat content

The fat content of texturized protein was found to be 4.03% **(Table 4.7)**. This fat content was within the range observed for texturized vegetable protein (5.45%) used as reference material. The fat content of texturized proteins can vary significantly depending on the protein source and processing methods. For instance, TVPs produced from pea proteins have significantly higher fat content, averaging around 6.0%, compared with textured soy proteins or wheat gluten, which had lower fat content averages of 2.7% and 2.8%, respectively (Hong et al., 2022). The fat content of texturized protein products is an important consideration that has implications for both nutritional value and sensory characteristics. A fat content of 4.03% in texturized protein suggests a moderate level of fat, which can contribute to various aspects of the product's quality and performance. Fat can impart a juicy, tender, and slightly moist quality, which can enhance the overall eating experience and make the product more akin to traditional meat-based products (Ketnawa & Rawdkuen, 2023). Additionally, fat can act as a carrier for flavour compounds, potentially enhancing the perception of taste and aroma in the final product. This can be particularly important for plant-based protein sources, which may have inherent off-flavours or require additional seasoning and flavouring to achieve a desirable taste profile (Anjum et al., 2011).

4.3.9.1.4. Protein content

The exceptionally high protein content of 64.12% **(Table 4.7)** in the optimized texturized protein represents a remarkable achievement in plant-based protein concentration technology, demonstrating more than double the protein density compared to the reference TVP material (30.11%), which signifies substantial advancement in processing efficiency and nutritional optimization (Hong et al., 2022). This dramatic protein enhancement was attributed to the strategic use of defatted Manila tamarind flour for protein isolate preparation, where lipid removal concentrates the protein fraction while eliminating components that could interfere with protein functionality, texturization, and storage stability (do-Carmo et al., 2023). The commercial significance of this 64.12% protein content cannot be overstated, as it positions the product in the premium protein supplement category, competing directly with animal-based proteins (typically 70-90% protein) while offering plant-based advantages such as sustainability, allergen considerations, and digestibility profiles that appeal to health-conscious consumers (Kinsella, 2018). From a nutritional standpoint, this high protein concentration ensures optimal amino acid density per serving, critical for meeting daily protein requirements efficiently while minimizing caloric intake from non-protein sources, particularly important for athletic nutrition, weight management, and therapeutic dietary applications (Laugesen et al., 2022). The functional implications are equally significant, as higher protein content typically correlates with improved gelation properties, water-binding capacity, and thermal stability during food processing, enabling superior texture development and structural integrity in final food applications (Arueya et al., 2017). This protein concentration also addresses the growing market demand for clean-label, minimally processed plant proteins that can replace traditional animal proteins without compromising nutritional adequacy or functional performance. The optimization process achieving this protein level while maintaining desirable textural and sensory properties represents a critical breakthrough in food technology, as many high-protein extraction methods often compromise taste, texture, or processing functionality, making this balanced achievement particularly valuable for commercial food formulations targeting the expanding plant-based protein market segment.

4.3.9.2.TPC, TFC and DPPH free radical scavenging activity

The antioxidant profile of the optimized texturized protein, characterized by TPC (1.52 mg GAE/g), TFC (1.29 mg QE/g), and DPPH scavenging activity (39.83% inhibition), represents a significant nutritional advancement over the reference TVP sample, demonstrating 7.8%, 104.8%, and 27.6% improvements respectively **(Table 4.7**), which collectively indicate enhanced bioactive compound retention during processing optimization. The TPC value of 1.52 mg GAE/g is particularly significant because phenolic compounds serve as primary defence mechanisms against lipid peroxidation, protein oxidation, and DNA damage caused by reactive oxygen species, making this moderate concentration valuable for both product stability and consumer health benefits (Grasso et al., 2019). The remarkable doubling of TFC from 0.63 to 1.29 mg QE/g **(Table 4.7**) was especially noteworthy because flavonoids possess specific biological activities including anti-inflammatory, cardio-protective, and neuroprotective properties that extend beyond general antioxidant capacity, positioning this texturized protein as a functional food ingredient rather than merely a protein source (Laugesen et al., 2022). The DPPH free radical scavenging activity of 39.83% represents practical antioxidant efficacy under standardized testing conditions, indicating that the product can neutralize approximately 40% of free radicals in the assay system, which translates to measurable protective effects against oxidative stress in biological systems (Palanisamy et al., 2019). These antioxidant parameters are significant in many ways because they contribute towards natural preservation properties, potentially reducing the need for synthetic antioxidants in food formulations while extending shelf life through prevention of rancidity and color degradation (Grasso et al., 2019). The retention and enhancement of these bioactive compounds during texturization processing suggested optimized extraction and processing conditions that preserve heat-sensitive phenolic and flavonoid structures, which is technically challenging given the high-temperature, high-shear conditions typical in protein texturization (Ketnawa & Rawdkuen, 2023). From a market perspective, these antioxidant values support premium positioning of the product in the functional food sector, where consumers increasingly seek plant-based proteins that provide additional health benefits beyond basic nutrition, making the documented antioxidant capacity a valuable marketing and nutritional differentiator in the competitive plant protein market.

Total Phenolic Content (TPC), Total Flavonoid Content (TFC) and DPPH free radical scavenging activity of the texturized protein were measured as 1.52 mg GAE/g, 1.29 mg QE/g, and 39.83 % inhibition, respectively **(Table 4.7**) and the values were a bit higher than that of the reference sample. The values of TPC, TFC and DPPH free radical scavenging activity for the reference sample (TVP) were 1.41 mg GAE/g, 0.63 mg QE/g, and 31.2% inhibition, respectively **(Table 4.7)**. A higher TPC value for the sample suggests a greater ability to combat oxidative stress and protect against cell damage. In this case, the TPC value of 1.52 mg GAE/g indicates a moderate concentration of phenolic compounds in the texturized protein. Otherwise, a higher TFC value signifies a higher concentration of flavonoids, which are beneficial for health (Grasso et al., 2019). The TFC value of 1.29 mg QE/g suggests a moderate level of flavonoids in the texturized protein. In conclusion, the TPC and TFC values of 1.52 mg GAE/g and 1.29 mg QE/g, respectively, demonstrate the antioxidant potential of the texturized vegetable protein due to the presence of phenolic compounds and flavonoids (Palanisamy et al., 2019). These compounds serve a crucial part in protecting cells from oxidative damage and promoting overall health and well-being (Ketnawa & Rawdkuen, 2023).

4.3.9.3. Colour parameters

The colour values of the optimized texturized protein are shown in **Table 4.8**. The *L** value of the texturized protein was measured at 57.25 which was quite comparable with the *L** value (56.61) of the reference material. Comparable outcomes were stated by Chiang et al. (2019) during their research on effects of soy protein to wheat gluten ratio on the physicochemical characteristics of meat substitutes that were extruded. They reported the *L** values of the extruded meat analogues in the range of 58.01 to 61.44. The *a** value of the sample was measured as 6.98 indicating a shift towards redness in the colour of the sample and it very much comparable to the *a** value of reference sample (6.21). Lee et al. (2022) reported similar findings for the extruded meat analogues with their *a** values in the range of 6.46 to 8.41. The *b** value of the sample was 21.74 which was a bit lower than that of reference material (27.56). The results were significantly in accordance with the reports of Lee et al. (2022) as the *b** values of extruded meat analogues ranged from 16.76 to 23.90. The color of texturized proteins is important because consumers recognize it as the first appearance characteristic and their buying behaviour depends too much on it. A visually appealing color, similar to that of real

meat, can enhance the appeal of plant-based alternatives and help consumers overcome any hesitation in trying these products.

Table 4.8: Colour and textural properties of the texturized protein

Parameters		Freeze texturized protein	Texturized soy-protein*
Color Properties	***L****	57.25±0.92^{a}	56.61±0.86^{b}
	a*	6.98±0.16^{a}	6.21±0.28^{b}
	b*	21.74±0.30^{b}	27.56±0.52^{a}
Hardness (g)		481.08±1.02^{b}	625.3±3.46^{a}
Springiness		0.69±0.02^{b}	0.85±0.01^{a}
Cutting force vertical (F_V) (g)		684.9±5.26^{b}	986.4±6.70^{a}
Cutting force parallel (F_L) (g)		972.55±8.14^{b}	1435.7±10.24^{a}
Degree of texturization (DT= F_L/ F_V)		1.42±0.02^{b}	1.45±0.02^{a}

Values are expressed as the average of triplicates ±SD. Different superscripts within the same row are significantly different ($p<0.05$) (* Signifies reference sample)

4.3.10. Characterization of functional properties

4.3.10.1. Cooking yield and cooking loss

The cooking yield of the texturized protein was found to be 86.33%, while the cooking loss was 13.67% **(Table 4.7)**. In comparison, the cooking yield of the reference material was found to be 90.33%, while the cooking loss was 9.67% **(Table 4.7)**. The values indicate that the texturized protein exhibited good cooking properties, with a high yield and low loss during the cooking process. Cooking yield is an important parameter that reflects the protein's capacity to retain its structure including moisture content during cooking (Ketnawa & Rawdkuen, 2023). A high cooking yield is desirable as it suggests that the protein will maintain its texture and juiciness when incorporated into food products. The cooking yield of the texturized protein in this study is comparable to or higher than values reported for other texturized vegetable proteins, such as those made from soy, pea, or wheat gluten (Ketnawa & Rawdkuen, 2023; Hong et al., 2022) Cooking loss, on the other hand, represents the amount of moisture and fat that is lost from the protein during cooking (Chen et al., 2023). A low cooking loss is preferred as it

indicates that the protein will not become dry or tough when cooked. The cooking loss of 13.67% for the texturized protein is relatively low compared to values reported for other texturized proteins, which can range from around 2 to 35% (Samard et al., 2021). The extrusion process used to produce the texturized protein likely resulted in the creation of a stable protein matrix that can retain moisture and resist shrinkage during cooking. Overall, the cooking properties of the texturized protein suggest that it would be a suitable ingredient for use in various food applications, like meat substitutes or extruded snacks, where a high-quality texture and mouthfeel are desired (Chen et al., 2023).

4.3.10.2. Expressible moisture

The assessment of expressible moisture, which can affect the sensory qualities and additional processing processes needed to create final goods (such nuggets), is an indirect assessment of WHC. After pressing, there was reduced water loss (11.65%) in the freeze-textured protein **(Table 4.7)**. In comparison, the water loss from the reference sample was reported to be around 12.05% **(Table 4.7)**. The water loss was not significantly affected by freeze texturization temperature, in contrast to components like wheat gluten and jackfruit flour. When compared to other texturized proteins, the lower cutting force of the tested material showed that the water was trapped in the structure during pressing. Compact structures store water better than soft structures in protein-based systems. As a result, the hardness characteristic of the texturized protein had a significant impact on both the cooking yield and the expressible moisture. Similar results were reported by Samard & Ryu (2019) for the developed plant protein-based meat analogue who reported integrity index of 6.02% for soy-protein isolate along with 30.99% in case of wheat gluten-based meat analogue. In another research, integrity index of 13.53% (Gu & Ryu, 2017) and 12.87% (Gu & Ryu, 2018), respectively, were reported for texturized vegetable proteins. Integrity index refers to the residue texture or simply expressible moisture after the pellet TVP is hydrated, pressurized, homogenized, and dried.

4.3.10.3. *In-vitro* protein digestibility (IVPD)

IVPD was found to be 64.33% for optimized texturized protein **(Table 4.7)** which was comparatively lower than that of the reference material (TVP) which had IVPD values of 75.61%. This was probably due to greater breakdown of protein structures at higher

barrel temperatures in case of TVPs which results in enhancement of the protein digestibility (Palanisamy et al., 2019). *In-vitro* protein digestibility is a crucial parameter that reflects the extent to which proteins can be broken down into amino acids during digestion, indicating their bioavailability and nutritional quality. A digestibility of 64.33% suggests that a significant portion of the protein in the texturized protein can be effectively digested and absorbed by the body (Kiiru, 2020). The protein digestibility of texturized proteins is impacted by numerous factors, including the protein source, processing means, and structural changes induced during texturization. The optimization process likely aimed to enhance the protein digestibility of the texturized protein while maintaining its desirable textural and functional properties (Samard et al., 2021). Achieving a protein digestibility of 64.33% indicates that the texturized protein can serve as a valuable source of digestible protein in food products. Moreover, the in-vitro protein digestibility value of 64.33% aligns with the protein digestibility values reported for other texturized vegetable proteins, highlighting the potential of the optimized texturized protein as a nutritious and bioavailable plant-based protein source (Chen et al., 2023). This finding underscores the importance of optimizing processing parameters to enhance the digestibility and overall nutritional quality of texturized proteins for various food applications. One possible explanation for higher protein digestibility values is the modification of proteins due to treatment and the high-quality protein (Grasso et al., 2019). This result is corroborated by studies of Azzollini et al. (2017), which reported an enhancement in *in-vitro* protein digestibility for wheat-based extruded products.

4.3.11. Structural and morphological characterization

4.3.11.1. Characterization of textural properties: Cutting force and degree of texturization (DT)

The hardness of the texturized protein was measured at 481.08 g **(Table 4.8)**. Cutting force is an indirect measurement of hardness, fibrous structure development, or degree of texturization. In the current study, the cutting force of the texturized protein was measured as 684.9 g (6.85 N) for vertical cutting force (F_V) and 972.55 g (9.72 N) as parallel cutting force (F_L), and the results are shown in **Table 4.8**. In comparison, the hardness of the reference material was 625.3 g and its vertical cutting force and parallel cutting force were measured as 986.4 and 1435.7 g, respectively **(Table 4.8)**. The addition of liquid (water and oil) had a significant effect on the cutting force of the

texturized protein. In one study on extrusion of texturized protein, Fang et al. (2014) demonstrated that a rise in feed water can cause incomplete protein denaturation and unfolding, resulting in lower protein texturization and cutting force. Variations in the water concentration in the sample had a significant impact on the cutting force, which is directly related with the hardness of the samples. This demonstrates that the water concentration is an important parameter for texturization. The creation of fibrous matrix is indicated by the degree of texturization (DT), which should show a dimensionless value greater than one. This is because cutting through the sample requires more force since cutting through the parallel fibre network (F_L) requires greater resistance than cutting through the vertical fibre network (F_V). The degree of texturization of the texturized protein was 1.42 and that of the reference material was 1.45. The outcomes were in agreement with the results of Chiang et al. (2019) where degree of texturization of the extruded soy-based meat analogues ranged from 1.3 to 1.74. The degree of fibrousness and texturization, as well as hardness, can affect how well the meat analogues are perceived by the senses. Palanisamy et al. (2018) observed the extrudates with a cutting force of approximately 926 g (9.26 N) are sensorically more palatable than soya meat analogues with cutting forces ranging from 785 to 1039 g (7.85 to 10.39 N). Higher cutting force may be preferable owing to better texturization, but the sensory acceptability of a product that is overly hard may be compromised. For the purpose of choosing the appropriate texturization parameters, it is crucial to take into account both the features of hardness and texturization.

4.3.11.2. Morphological properties by scanning electron microscopy (SEM)

Scanning electron micrographs of the freeze-texturized protein is shown in **Figure 4.5**. From the SEM micrographs, it can be clearly seen that layered structure was observed for freeze-texturized protein **(Figure 4.5 (i), (ii), (iii), (iv))** and the fiber size ranged between 10-100 μm, with various segmented layers observed for texturized protein at higher magnifications. The microstructural analysis revealed that the developed protein samples exhibited fibrous architecture closely resembling that of commercial texturized vegetable protein (TVP), which served as the reference standard, with fiber dimensions consistently ranging between 10-150 μm as documented in **Figure 4.6 (i), (ii), (iii), (iv).** These findings aligned with previous researches by Krintiras et al. (2015), who investigated the development of plant-based meat analogues using wheat gluten and soy

protein combinations and reported the formation of large, well-defined fibrous matrices in meat substitute formulations containing 20% wheat gluten. However, they also pointed that increasing wheat gluten content to 30% resulted in a more complex microstructure characterized by the presence of numerous smaller secondary fibers interspersed throughout the primary fibrous network, suggesting that protein concentration significantly influences the final textural architecture of PBMAs.

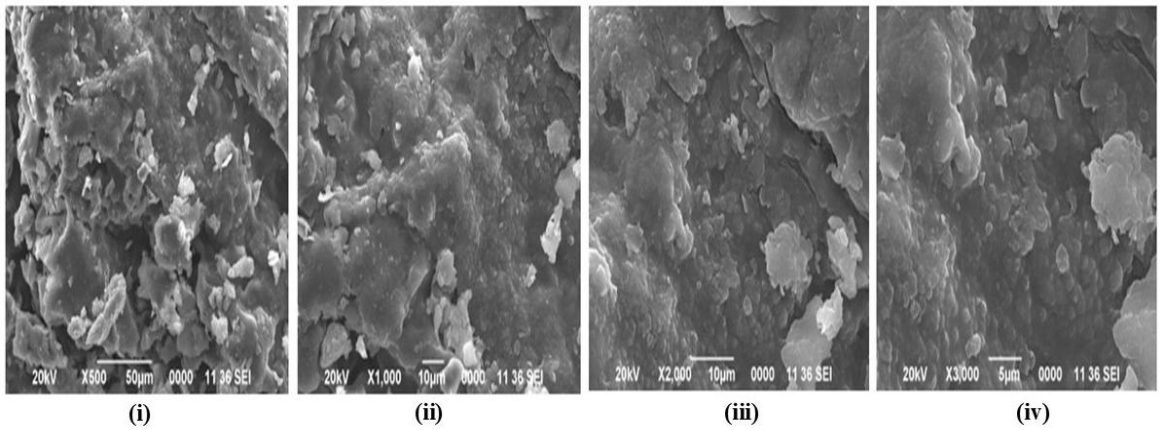

Figure 4.5: Scanning electron micrographs of the freeze-texturized protein (sample) at different magnifications (500X, 1000X, 2000X, and 3000X)

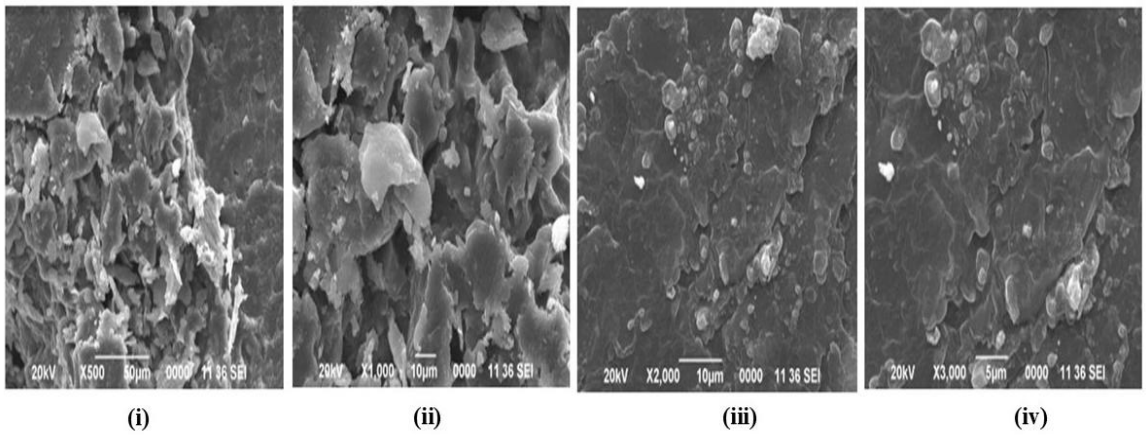

Figure 4.6: Scanning electron micrographs of the texturized vegetable protein (reference) at different magnifications (500X, 1000X, 2000X, and 3000X)

The anisotropic microstructural characteristics observed in the texturized protein, resulting from optimized protein isolate (PI) and wheat gluten (WG) levels, represent a critical achievement in plant-based meat analogue technology, as these fibrous structures directly correlate with the directional mechanical properties essential for replicating the

muscle fiber alignment found in animal meat products (Dekkers et al., 2018). The development of these oriented fibrous microstructures is fundamentally significant because anisotropy, the directional dependence of material properties, enables the texturized protein to exhibit differential resistance to mechanical stress along different axes, mimicking the characteristic "grain" and bite resistance that consumers associate with authentic meat texture (Samard & Ryu, 2019). The correlation between increased PI and WG concentrations and enhanced fibrous structure formation indicates successful protein network development, where wheat gluten's viscoelastic properties provide structural framework while protein isolates contribute to gel strength and water-binding capacity, creating the complex three-dimensional matrix necessary for meat-like texture development. The comparative analysis with findings of Samard & Ryu (2019) using various plant proteins (soy, mung bean, peanut, pea) validated the microstructural approach, while highlighting that protein source selection significantly influences air cell formation and distribution patterns, with non-uniform air cell structures contributing to the sponge-like texture that affects mouthfeel, juiciness perception, and overall sensory acceptance (Kyriakopoulou et al., 2019). The presence of higher quantities of air cells with non-uniform distribution is functionally important because these void spaces facilitate moisture retention, sauce absorption, and textural contrast during mastication, essential characteristics for consumer satisfaction in plant-based meat applications. Corroborating research on methylcellulose and enzymatically modified plant fiber binding systems by Wei et al. (2024) further validated the microstructural approach, demonstrating that consistent surface morphology achieved through citrus fiber fortification can enhance structural integrity and visual appeal at high magnification levels. The significance of achieving these specific microstructural features extends beyond texture to encompass cooking behaviour (Samard & Ryu, 2019). This is because anisotropic structures influence heat transfer, moisture migration, and protein coagulation patterns during thermal processing, ultimately determining the final product's performance in various culinary applications and cooking methods typical of meat-based dishes.

4.4. Comparison of the texturized proteins developed by different methods

Figure 4.7 shows the overall methodology used for texturization of Manila tamarind seed protein by adopting two different processing methods, freeze texturization and

freeze structuring. The texturized proteins are then subjected to complete characterization in the form of physicochemical analysis, visual appearance determination, texture profile analysis, texturization degree assessment, cooking properties measurement, and expressible moisture content determination, with the reference standard being commercial texturized soy protein (TSP) and all the parameters being compared on that basis to assess the effectiveness and quality of plant-based protein alternatives developed.

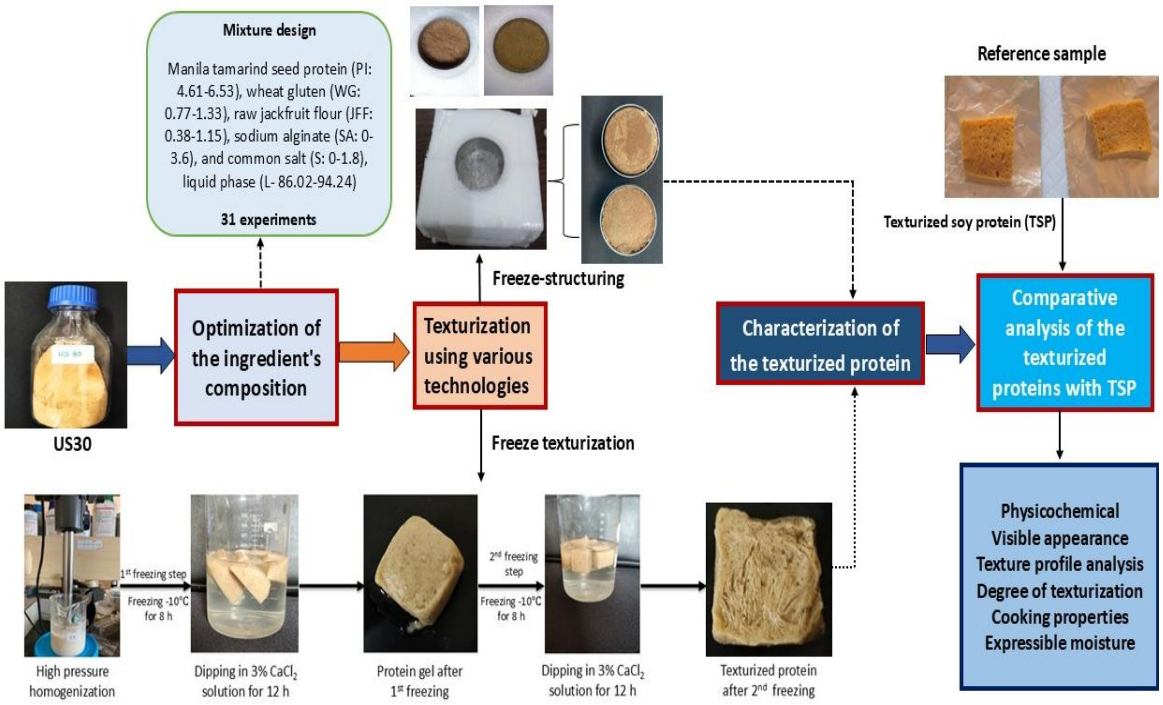

Figure 4.7: Flowchart depicting the steps used in the formulation of the texturized proteins prepared through freeze texturization and freeze structuring and comparison of their quality parameters with texturized soy protein (reference sample)

4.4.1. Appearance

The comparative visual analysis presented in **Figure 4.8** provides comprehensive documentation of structural development mechanisms in protein-based meat analogues produced through distinct freeze texturization and freeze structuring methodologies. The image effectively demonstrates how different processing techniques significantly influence both surface morphology characteristics and internal fiber alignment patterns in the final texturized products, as extensively documented by Ketnawa & Rawdkuen

(2023). In the freeze texturization process illustrated in **Figure 4.8 A**, the samples were systematically examined at two critical developmental stages corresponding to post-first and post-second freezing cycles, revealing progressive structural evolution throughout the processing sequence. The cross-sectional microscopic images obtained following the initial freezing cycle clearly demonstrates the formation of a relatively coarse and discontinuous fibrous network structure, which suggests the early development of oriented protein structures resulting from controlled directional ice crystal formation and subsequent protein matrix reorganization (Chantanuson et al., 2022). Following completion of the second freezing cycle, the fibrous structures undergo significant architectural development, exhibiting enhanced layering characteristics and partial fiber alignment that becomes clearly visible in cross-sectional analysis, indicating progressive protein matrix organization and improved structural integrity. This sequential structural development demonstrates the cumulative effect of repeated freeze-thaw cycles on protein network formation, where each processing stage contributes to the overall textural complexity and fibrous architecture that closely mimics the characteristic properties of conventional meat products.

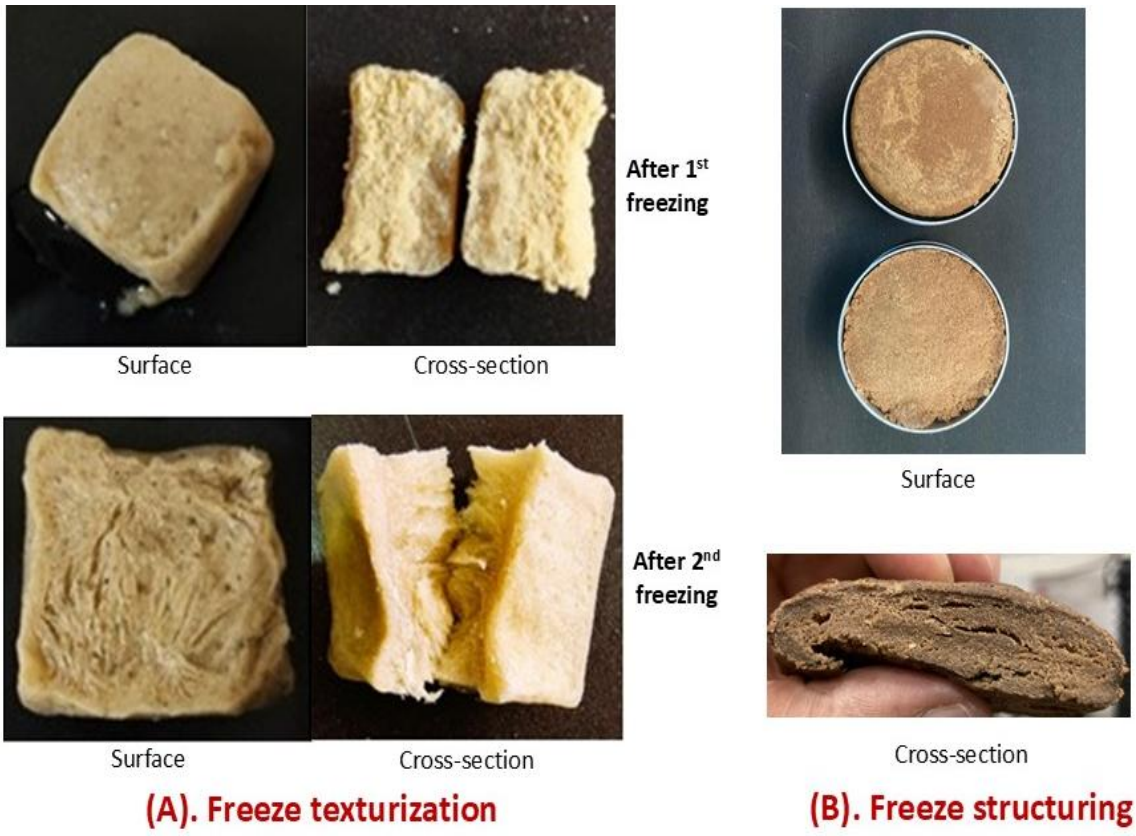

Figure 4.8: Visual appearance of the texturized proteins prepared through freeze texturization (A) and freeze structuring (B)

This suggests repeated freeze-thaw cycles enhance anisotropic structuring by facilitating ice crystal growth and protein aggregate realignment, improving fiber formation through phase separation and protein entrapment (Chiang et al., 2019). Freeze structuring **(Figure 4.8 B)** yields different results, the surface view displays a uniform, compact structure, while cross-sections show densely layered fibrous networks resembling cooked meat tissues. This effect stems from directional freezing during freeze structuring, creating aligned ice crystals that template the protein network during thawing and drying (Webb et al., 2023). The fibrous structure in freeze texturization appears more coherent and anisotropic compared to freeze structuring. Such morphology plays a critical role in replicating meat-like textures in plant-based alternatives, with structural anisotropy contributing to chewiness, juiciness, and bite resistance (Yong et al., 2020). These observations confirm that while both freeze-induced methods contribute to fibrous development, freeze texturization offers superior architectural organization and functional mimicry of animal meat, making it more promising for high-fidelity meat analogue production (Chantanuson et al., 2022).

4.4.2. Physicochemical and functional properties of the texturized proteins

Table 4.9 gives a comparative analysis of physicochemical and functional properties across three texturized protein types: freeze-structured, freeze-texturized, and commercial texturized soy protein (TSP). The data revealed notable variations in moisture content, protein composition, color attributes, cooking performance, and water retention, factors critical to sensory and functional performance of meat analogues. Moisture content, which affects juiciness and mouthfeel, measured significantly ($p<0.05$) lower in freeze-structured samples (36.58%) versus freeze-texturized (45.93%) and TSP (44.53%). This indicates a denser, less hydrated matrix in freeze-structured products, likely from stronger protein networks binding less free water (Samard & Ryu, 2019). Protein content was highest in freeze-texturized samples (64.12% d.b.), followed by freeze-structured (54.91% d.b.), and lowest in TSP (30.11% d.b.). Such elevated protein levels in experimental samples, particularly freeze-texturized, suggest enhanced protein retention, potentially reflecting more efficient formulation during processing (Webb et al., 2023). Color properties serve as important indicators of consumer acceptance and perceived meat similarity (Zhou et al., 2022). Freeze-texturized samples showed highest lightness (L^*) value of 57.25, followed by TSP (56.61) and freeze-

structured protein (48.13), suggesting the latter possessed darker appearance, possibly from protein denaturation or Maillard reactions during processing.

Table 4.9: Physicochemical and functional properties of the texturized proteins

Parameters		**Freeze structured**	**Freeze texturized**	**Texturized soy-protein***
Moisture (%)		36.58±0.40^{c}	45.93±0.17^{a}	44.53±0.36^{b}
Protein (% d.b.)		54.91±0.68^{b}	64.12±0.35^{a}	30.11±0.17^{c}
Color Properties	***L****	48.13±0.08^{c}	57.25±0.92^{a}	56.61±0.86^{b}
	a*	4.80±0.02^{c}	6.98±0.16^{a}	6.21±0.28^{b}
	b*	11.05±0.30^{c}	21.74±0.30^{b}	27.56±0.52^{a}
Cooking Yield (%)		78.46±1.25^{c}	86.33±0.98^{b}	90.33±0.74^{a}
Expressible Moisture (%)		8.38±0.06^{c}	11.65±0.13^{b}	12.05±0.05^{a}

Values are expressed as the average of triplicates ± SD. Different superscripts within the same row are significantly different ($p < 0.05$) (* Signifies reference sample)

Similarly, redness (*a**) and yellowness (*b**) values measured lowest in freeze-structured proteins (4.80 and 11.05) and highest in TSP (6.21 and 27.56). These differences may influence visual perception of meat resemblance, with freeze-texturized products potentially appearing more meat-like in coloration (Webb et al., 2023). Cooking yield and expressible moisture represent crucial functional indicators reflecting structural integrity and water-holding capacity (Zhou et al., 2022). Cooking yield was lowest in freeze-structured protein (78.46%) and highest in TSP (90.33%), demonstrating superior water and fat retention during thermal processing in the reference sample. Freeze-texturized protein showed intermediate performance (86.33%), outperforming freeze-structured protein. Similarly, expressible moisture, measuring free water expulsion under pressure, was lowest in freeze-structured protein (8.38%), indicating a tightly bound matrix with reduced water mobility. Freeze-texturized and TSP samples exhibited higher values (11.65% and 12.05%), suggesting greater juiciness but potentially looser structural networks (Patel and Yamamoto, 2023). In similar studies, high-moisture

extruded soy protein analogues typically exhibit protein content between 30–50% (d.b.), cooking yields of 85–95%, and expressible moisture ranging from 10–13%, depending on formulation and process variables (Fang et al., 2014; Dekkers et al., 2018). Another study examining freeze-aligned pea protein networks reported similar reduction in L^* values due to browning and increased chewiness and cohesiveness compared to isotropic structures (Zhou et al., 2022). This dataset supports the conclusion that freeze-texturization delivers superior protein enrichment and cooking yield, while freeze-structuring provides a more compact, water-retentive matrix, both representing meaningful advances over conventional texturized soy protein products (Dekkers et al., 2018).

4.4.3. Textural properties of the texturized proteins

Table 4.10 offers a thorough comparison of textural properties among texturized proteins developed through two experimental approaches, freeze structuring and freeze texturization, alongside a commercial texturized soy protein (TSP) reference. These parameters, assessed via Texture Profile Analysis (TPA) and cutting force measurements, provide valuable insights into mechanical behaviour, bite characteristics, and structural integrity of the protein alternatives. Hardness, indicating compression force requirements, showed the freeze-texturized sample had a moderate value of 481.08 g, positioned between TSP (625.3 g) and freeze-structured protein (307.70 g). This gradient suggests freeze texturization creates a firmer network than freeze structuring, yet remains less compact than industrial TSP (Zhou et al., 2022). Springiness, measuring shape recovery after deformation, followed a similar pattern: TSP demonstrated highest values (0.85), signifying strong elastic recovery, while freeze-texturized and freeze-structured samples showed progressively lower values (0.69 and 0.44) (Samard & Ryu, 2019). This indicates industrial TSP maintains mechanical resilience post-chewing more effectively, potentially due to optimized extrusion parameters. Conversely, cohesiveness, reflecting internal bonding strength during deformation, reached its peak in freeze-structured protein (0.17), slightly exceeding both TSP (0.119) and freeze-texturized protein (0.113), which suggests a stronger inter-particle network, though less flexible (Zhang et al., 2023). Resilience, representing energy recovery capability after deformation, revealed marked differences: freeze-structured protein recorded the highest resilience (0.73), while freeze-texturized and TSP showed minimal values (0.023 and

0.014) (Zhou et al., 2022).

Table 4.10: Textural properties of the texturized proteins along with reference sample

Parameters	Freeze structured protein	Freeze texturized protein	Texturized soy-protein*
Hardness (g)	307.70 ± 4.07^{b}	481.08 ± 1.02^{c}	625.3 ± 3.46^{a}
Springiness (%)	0.44 ± 0.06^{c}	0.69 ± 0.02^{b}	0.85 ± 0.01^{a}
Cohesiveness	0.17 ± 0.01^{a}	0.113 ± 0.01^{b}	0.119 ± 0.01^{b}
Resilience	0.73 ± 0.04^{a}	0.023 ± 0.01^{b}	0.014 ± 0.01^{c}
Fracturability (g)	-	-	-
Adhesiveness (g.s)	40.55 ± 0.14^{b}	37.68 ± 0.11^{c}	91.02 ± 0.10^{a}
Gumminess (g)	52.30 ± 0.69^{a}	20.46 ± 0.23^{c}	50.61 ± 0.58^{b}
Chewiness (g)	23.14 ± 0.02^{b}	14.11 ± 0.04^{c}	43.01 ± 0.09^{a}
Cutting Force vertical (F_V) (g)	1173.80 ± 8.75^{a}	684.9 ± 5.26^{c}	986.4 ± 6.70^{b}
Cutting force parallel (F_L) (g)	1250.60 ± 6.54^{b}	972.55 ± 8.14^{c}	1435.7 ± 10.24^{a}
Degree of texturization ($DT = F_L/ F_V$)	1.06 ± 0.04^{b}	1.42 ± 0.02^{a}	1.45 ± 0.02^{a}

Values are expressed as the average of triplicates ± SD. Different superscripts within the same row are significantly different ($p < 0.05$) (* Signifies reference sample)

These findings indicate freeze structuring yields a more elastic or gel-like texture, potentially suitable for applications requiring rapid deformation recovery (Bakhsh et al., 2021). Adhesiveness, measuring work required to overcome attractive forces between sample and probe, was highest in TSP (91.02 g.s), indicating a sticky texture likely resulting from increased moisture mobility or surface protein interactions (Chen et al., 2023). Freeze-structured and freeze-texturized samples exhibited significantly lower adhesiveness (40.55 and 37.68 g.s), potentially contributing to cleaner mouthfeel perception (Dekkers et al., 2018). Gumminess and chewiness, key indicators of texture perception during mastication, further supported these observations. Freeze-structured protein displayed highest gumminess (52.30 g), suggesting greater resistance under compression despite lower hardness values. Freeze-texturized samples were least gummy

(20.46 g), possibly due to their reduced cohesive structure (Zhang et al., 2023). Similarly, chewiness measurements positioned TSP as most chewy (43.01 g), followed by freeze-structured (23.14 g) and freeze-texturized (14.11 g) proteins, suggesting freeze-structured samples provided more meat-like chew compared to freeze-texturized alternatives (Chantanuson et al., 2022). Cutting forces in vertical (F_V) and parallel (F_L) orientations assessed anisotropy in structural alignment across samples. Highest F_V and F_L values appeared in TSP (986.4 g and 1435.7 g), demonstrating superior structural resistance. Freeze-texturized samples required lowest cutting forces (684.9 g F_V, 972.55 g F_L), suggesting a softer, less fibrous matrix, while freeze-structured protein showed intermediate mechanical characteristics (Zhou et al., 2022). Notably, degree of texturization (DT) was comparable between TSP (1.45) and freeze-texturized samples (1.42), both exceeding freeze-structured protein (1.06), indicating directional fiber alignment, a critical meat analogue attribute, was best replicated in freeze-texturized samples (Chantanuson et al., 2022).

For contextual comparison, research examining high-moisture extruded meat analogues reported chewiness values of 40–70 g and springiness approximately 0.8–0.9 for soy- or wheat-based systems (Dekkers et al., 2018), while studies on 3D-printed pea protein gels demonstrated DT values ranging from 1.2 to 1.5 depending on freezing orientation, closely aligning with freeze-texturized values observed here (Chen et al., 2023). Overall, freeze texturization effectively replicated key mechanical properties of commercial meat analogues while offering reduced chew resistance and cleaner mouthfeel, whereas freeze structuring excelled in resilience and cohesive network formation (Chen et al., 2023).

4.5. Conclusion

The present investigation utilized the freezing technique to generate porous arrangements with anisotropic layers and modulate the rheological characteristics of food gels derived from Manila tamarind seed protein. The freezing rate and duration have an impact on the structures that were produced, meaning that these parameters must be optimized in order to build a scalable method. D-optimal mixture design was utilized for optimizing the composition of the different components suitable for structuring and identifying an appropriate mixture composition to achieve the desired goal. The optimized formulation was then prepared using both freeze-texturization and freeze-structuring methods. The

formulation containing protein isolate at 6.53%, wheat gluten at 1.23%, jackfruit flour at 1.15%, sodium alginate at 3.6%, and liquid fraction (water/sunflower oil) at 87.48% produced the best results. The physicochemical, functional, and structural properties of the texturized proteins were analyzed and compared with a commercial texturized soy protein sample. The freeze-texturized protein showed superior protein content (64.125% db), cooking yield (86.33%), and degree of texturization (1.42) compared to the freeze-structured protein (1.06) and significant potential for use as a plant-based alternative, while the freeze-structured protein had a more compact and water-retentive matrix. Both methods produced texturized proteins with properties comparable to or better than the commercial reference sample. Furthermore, the presence of phenolic compounds and flavonoids demonstrated potential health benefits, while the fibrous microstructure suggested a promising meat-like texture. The evaluation of the optimized formulation upheld the effectiveness of the selected constituents in achieving the desired product attributes. Overall, the present research emphasizes the potential of plant-based proteins as a sustainable and nutritionally valuable substitute for animal-derived products.

References

Abdullah, F. A. A., Dordevic, D., Kabourkova, E., Zemancová, J., & Dordevic, S. (2022). Antioxidant and sensorial properties: Meat analogues versus conventional meat products. *Processes*, *10*(9), 1864.

AOAC. (2006). Official Methods of Analysis, 18th ed. *Association of Official Analytical Chemists*, Arlington, *VA, USA*.

Arora, S., Kataria, P., Nautiyal, M., Tuteja, I., Sharma, V., Ahmad, F., & Gupta, A. K. (2023). Comprehensive review on the role of plant protein as a possible meat analogue: Framing the future of meat. *ACS Omega*, *8*(26), 23305-23319.

Anjum, F. M., Naeem, A., Khan, M. I., Nadeem, M., & Amir, R. M. (2011). Development of texturized vegetable protein using indigenous sources. *Pakistan Journal of Food Science*, *21*(1-4), 33-44.

Arueya, G., Owosen, B., & Olatoye, K. (2017). Development of Texturized Vegetable Protein from Lima bean (*Phaseolus lunatus*) and African oil bean seed [*Pentaclethrama crophylla* (Benth)]: optimization approach. *Acta Universitatis Cinbinesis, Series E: Food Technology*, *21*(1).

Azzollini, D., Derossi, A., Fogliano, V., Lakemond, C. M. M., & Severini, C. (2017). Effects of formulation and process conditions on microstructure, texture and digestibility of extruded insect-riched snacks. *Innovative Food Science and Emerging Technologies*, *45*, 344–353.

Bakhsh, A., Lee, S. J., Lee, E. Y., Sabikun, N., Hwang, Y. H., & Joo, S. T. (2021). A novel approach for tuning the physicochemical, textural, and sensory characteristics of plant-based meat analogues with different levels of methylcellulose concentration. *Foods*, *10*(3), 560.

Chantanuson, R., Nagamine, S., Kobayashi, T., & Nakagawa, K. (2022). Preparation of soy protein-based food gels and control of fibrous structure and rheological property by freezing. *Food Structure*, *32*, 100258.

Chen, D., Jones, O. G., & Campanella, O. H. (2023). Plant protein-based fibers: Fabrication, characterization, and potential food applications. *Critical Reviews in Food Science and Nutrition*, *63*(20), 4554-4578.

Chiang, J. H., Loveday, S. M., Hardacre, A. K., & Parker, M. E. (2019). Effects of soy protein to wheat gluten ratio on the physicochemical properties of extruded meat analogues. *Food Structure*, *19*, 100102.

Consolacion, F. I., & Jelen, P. (1986). Freeze-texturization of proteins: Effect of the alkali, acid and freezing treatments on texture formation. *Food Structure*, *5*(1), 5.

Cui, B., Mao, Y., Liu, J., Liang, X., Wu, D., Chen, X., & Li, B. (2023). Effect of salt on solution behavior of spinning medium and properties of meat analogue fibers. *Food Hydrocolloids*, *139*, 108540.

Cui, B., Zeng, X., Liang, H., Li, J., Zhou, B., Wu, D., & Li, B. (2024). Construction of a soybean protein isolate/polysaccharide-based whole muscle meat analogue: Physical properties and freeze-thawing stability study. *International Journal of Biological Macromolecules*, 131037.

Dekkers, B. L., Boom, R. M., & van der Goot, A. J. (2018). Structuring processes for meat analogues. *Trends in Food Science and Technology*, *81*, 25-36.

do-Carmo, C. S., Rieder, A., Varela, P., Zobel, H., Dessev, T., Nersten, S., & Knutsen, S. H. (2023). Texturized vegetable protein from a faba bean protein concentrate and an oat fraction: Impact on physicochemical, nutritional, textural and sensory properties. *Future Foods*, *7*, 100228.

Dutta, D., & Sit, N. (2023). Comparison of properties of films prepared from casein modified by ultrasound and autoclave treatment. *Journal of Food Measurement and Characterization*, *17*(5), 5426-5439.

El Youssef, C., Bonnarme, P., Fraud, S., Péron, A. C., Helinck, S., & Landaud, S. (2020). Sensory improvement of a pea protein-based product using microbial co-cultures of lactic acid bacteria and yeasts. *Foods*, *9*(3), 349.

Fang, Y., Zhang, B., & Wei, Y. (2014). Effects of the specific mechanical energy on the physicochemical properties of texturized soy protein during high-moisture extrusion cooking. *Journal of Food Engineering*, *121*, 32-38.

Feili, R., Zzaman, W., Abdullah, W. N. W., & Yang, T. A. (2013). Physical and sensory analysis of high fiber bread incorporated with jackfruit rind flour. *Food Science and Technology*, *1*(2), 30-36.

Grasso, S., Smith, G., Bowers, S., Ajayi, O. M., & Swainson, M. (2019). Effect of texturized soy protein and yeast on the instrumental and sensory quality of hybrid beef meatballs. *Journal of Food Science and Technology*, *56*, 3126-3135.

Hamid, M. A., Tsia, F. L. C., Okit, A. A. B., Xin, C. W., Cien, H. H., Harn, L. S., & Yee, C. F. (2020). The application of Jackfruit by-product on the development of healthy meat analogue. In *IOP Conference Series: Earth and Environmental Science*, *575*(1), 012001.

Hong, S., Shen, Y., & Li, Y. (2022). Physicochemical and functional properties of texturized vegetable proteins and cooked patty textures: Comprehensive characterization and correlation analysis. *Foods*, *11*(17), 2619.

Hsu, H. W., Vavak, D. L., Satterlee, L., & Miller, G. A. (1977). A multienzyme technique for estimating protein digestibility. *Journal of Food Science*, *42*(5), 1269-1273.

Ishaq, A., Irfan, S., Sameen, A., & Khalid, N. (2022). Plant-based meat analogues: A review with reference to formulation and gastrointestinal fate. *Current Research in Food Science*, *5*, 973-983.

Ketnawa, S., & Rawdkuen, S. (2023). Properties of Texturized Vegetable Proteins from Edible Mushrooms by Using Single-Screw Extruder. *Foods*, *12*(6), 1269.

Kiiru, S. M. (2020). *In vitro protein digestibility and textural properties of high moisture extruded cricket-soy meat analogues* (Doctoral dissertation, JKUAT-AGRICULTURE).

Kinsella, J. E. (2018). Protein texturization fabrication and flavoring. In *Handbook of nutritional supplements* (pp. 35-106). CRC Press.

Krintiras, G. A., Göbel, J., Van der Goot, A. J., & Stefanidis, G. D. (2015). Production of structured soy-based meat analogues using simple shear and heat in a Couette Cell. *Journal of Food Engineering*, *160*, 34-41.

Kurek, M. A., Onopiuk, A., Pogorzelska-Nowicka, E., Szpicer, A., Zalewska, M., & Półtorak, A. (2022). Novel protein sources for applications in meat-alternative products—Insight and challenges. *Foods*, *11*(7), 957.

Kyriakopoulou, K., Dekkers, B., & van der Goot, A. J. (2019). Plant-based meat analogues. In *Sustainable meat production and processing* (pp. 103-126). Academic Press.

Laugesen, S. B., Dethlefsen, S. L., Petersen, I. L., & Aaslyng, M. D. (2022). Texturized Vegetable Protein as a Source of Protein Fortification of Wheat Buns. *Foods*, *11*, 3647.

Lee, E. J., & Hong, G. P. (2020). Effects of microbial transglutaminase and alginate on the water-binding, textural and oil absorption properties of soy patties. *Food Science and Biotechnology*, *29*, 777-782.

Lee, J. S., Oh, H., Choi, I., Yoon, C. S., & Han, J. (2022). Physico-chemical characteristics of rice protein-based novel textured vegetable proteins as meat analogues produced by low-moisture extrusion cooking technology. *LWT- Food Science and Technology*, *157*, 113056.

Lin, Q., Pan, L., Deng, N., Sang, M., Cai, K., Chen, C., & Ye, A. (2022). Protein digestibility of textured-wheat-protein (TWP)-based meat analogues:(I) Effects of fibrous structure. *Food Hydrocolloids*, *130*, 107694.

López, D. N., Ingrassia, R., Busti, P., Bonino, J., Delgado, J. F., Wagner, J., & Spelzini, D. (2018). Structural characterization of protein isolates obtained from chia (*Salvia hispanica* L.) seeds. *LWT- Food Science and Technology*, *90*, 396-402.

Nunes, Â. A., Favaro, S. P., Miranda, C. H., & Neves, V. A. (2017). Preparation and characterization of baru (*Dipteryx alata* Vog) nut protein isolate and comparison of its physico-chemical properties with commercial animal and plant protein isolates. *Journal of the Science of Food and Agriculture*, *97*(1), 151-157.

Palanisamy, M., Töpfl, S., Aganovic, K., & Berger, R. G. (2018). Influence of iota carrageenan addition on the properties of soya protein meat analogues. *Lwt*, *87*, 546-552.

Palanisamy, M., Töpfl, S., Berger, R. G., & Hertel, C. (2019). Physico-chemical and nutritional properties of meat analogues based on Spirulina/lupin protein mixtures. *European Food Research and Technology*, *245*, 1889-1898.

Pare, A. (2019). Effect of Soy-Jackfruit flour blend on the properties of developed meat analogues using response surface methodology. *International Journal of Pure and Applied Bioscience*, *7*(2), 600-610.

Rao, G. N., Nagender, A., Satyanarayana, A., & Rao, D. G. (2011). Preparation, chemical composition and storage studies of quamachil (*Pithecellobium dulce* L.) aril powder. *Journal of Food Science and Technology*, *48*, 90-95.

Rao, G. N. (2013). Physico-chemical, mineral, amino acid composition, in vitro antioxidant activity and sorption isotherm of *Pithecellobium dulce* L. seed protein flour. *Journal of Food and Pharmaceutical Sciences*, *1*(3).

Rosas Ulloa, P., Ulloa, J. A., Ulloa Rangel, B. E., & López Mártir, K. U. (2022). Protein Isolate from Orange (*Citrus sinensis* L.) Seeds: Effect of High-Intensity Ultrasound on Its Physicochemical and Functional Properties. *Food and Bioprocess Technology*, 1-14.
Samard, S., & Ryu, G. H. (2019). Physicochemical and functional characteristics of plant protein-based meat analogues. *Journal of Food Processing and Preservation*, *43*(10), e14123.

Samard, S., Maung, T. T., Gu, B. Y., Kim, M. H., & Ryu, G. H. (2021). Influences of extrusion parameters on physicochemical properties of textured vegetable proteins and its meatless burger patty. *Food Science and Biotechnology*, *30*, 395-403.

Sengar, A. S., Beyrer, M., McDonagh, C., Tiwari, U., & Pathania, S. (2023). Effect of Process Variables and Ingredients on Controlled Protein Network Creation in High-Moisture Plant-Based Meat Alternatives. *Foods*, *12*(20), 3830.

Sha, L., & Xiong, Y. L. (2020). Plant protein-based alternatives of reconstructed meat: Science, technology, and challenges. *Trends in Food Science and Technology*, *102*, 51-

61.

Sharma, H. K., Kaushal, P., & Singh, A. P. (2019). Rheological measurements of composite flour containing Jackfruit (Artocarpus heterophyllus Lam.) flesh flour and its identification by pattern recognition methods. *Journal of Food Measurement and Characterization*, *13*, 404-420.

Sofi, S. A., Singh, J., Muzaffar, K., Majid, D., & Dar, B. N. (2020). Physicochemical characteristics of protein isolates from native and germinated chickpea cultivars and their noodle quality. *International Journal of Gastronomy and Food Science*, *22*, 100258.

Taikerd, T., & Leelawat, B. (2023). Effect of young jackfruit, wheat gluten and soy protein isolate on physicochemical properties of chicken meat analogues. *Agriculture and Natural Resources*, *57*(2), 201-210.

Teng, C., & Campanella, O. H. (2023). A plant-based animal fat analogue produced by an emulsion gel of alginate and pea protein. *Gels*, *9*(5), 393.

Tuorila, H., & Hartmann, C. (2020). Consumer responses to novel and unfamiliar foods. *Current Opinion in Food Science*, *33*, 1-8.

Wani, I. A., Sogi, D. S., & Gill, B. S. (2015a). Physico-chemical and functional properties of native and hydrolysed protein isolates from Indian black gram (*Phaseolus mungo* L.) cultivars. *LWT-Food Science and Technology*, *60*(2), 848-854.

Wani, I. A., Sogi, D. S., Shivhare, U. S., & Gill, B. S. (2015b). Physico-chemical and functional properties of native and hydrolyzed kidney bean (*Phaseolus vulgaris* L.) protein isolates. *Food Research International*, *76*, 11-18.

Webb, D., Dogan, H., Li, Y., & Alavi, S. (2023). Physico-chemical properties and texturization of pea, wheat and soy proteins using extrusion and their application in plant-based meat. *Foods*, *12*(8), 1586.

Wei, A. S., Brishti, F. H., Sani, M. S. A., Ishamri, I., Sarbon, N. M., & Ismail-Fitry, M. R. (2024). Methylcellulose replacement with different enzymatically treated plant fibres as a binder in the production of plant-based meat patties. *LWT- Food Science and*

Technology, 116231.

Yong, H. I., Kim, T. K., Kim, Y. B., Jung, S., & Choi, Y. S. (2020). Functional and instrumental textural properties of reduced-salt meat emulsions with konjac gel: Combined effects of transglutaminase, isolate soy protein, and alginate. *International Journal of Food Properties*, *23*(1), 1296-1309.

Yuliarti, O., Kovis, T. J. K., & Yi, N. J. (2021). Structuring the meat analogue by using plant-based derived composites. *Journal of Food Engineering*, *288*, 110138.

Zeng, X., Cui, B., Zhou, B., Liang, H., Wu, D., Li, J., & Li, B. (2023). Effect of Ultrasound and Salt on Structural and Physical Properties of Sodium Alginate/Soy Protein Isolates Composite Fiber. *Foods*, *12*(23), 4275.

Zhang, R., Yang, Y., Liu, Q., Xu, L., Bao, H., Ren, X., & Jiao, A. (2023). Effect of wheat gluten and peanut protein ratio on the moisture distribution and textural quality of high-moisture extruded meat analogues from an extruder response perspective. *Foods*, *12*(8), 1696.

Zhou, H., Vu, G., Gong, X., & McClements, D. J. (2022). Comparison of the cooking behaviours of meat and plant-based meat analogues: Appearance, texture, and fluid holding properties. *ACS Food Science and Technology*, *2*(5), 844-851.